

SUPERGENE DISPERSION OF ANTIMONY AND A GEOCHEMICAL EXPLORATION MODEL FOR ANTIMONY ORE DEPOSITS

Glen Alfred Diemar



Supervisors: Peter Leverett & Peter A. Williams
School of Natural Sciences, University of Western Sydney
November 2008

This thesis is dedicated to my Mum and Dad

TABLE OF CONTENTS

Abstract	1
Statement of Authentication	3
Acknowledgements	4
Publications in Support of this Thesis	5
Chapter 1 Introduction	6
<i>Secondary Antimony Minerals</i>	7
<i>Simple Aqueous Antimony Chemistry</i>	12
Pourbaix Diagrams	12
Aqueous Species and Hydrolysis of Sb(III) and Sb(V)	15
Complex Formation with Geochemically Common Inorganic Ligands.....	18
<i>Antimony in Soils</i>	20
Chapter 2 Experimental	23
<i>Measurements</i>	23
<i>Syntheses</i>	24
Bottinoite and Brandholzite	24
Roméite and Bindheimite	24
Tripuhyite and an Fe(II)-Dominant Member of the Stibiconite Group	25
<i>Solubility Studies</i>	25
Bottinoite and Brandholzite	25
Roméite and Bindheimite	26
Mineral and Water Samples.....	26
Chapter 3 Field Sites and Settings	27
<i>Hillgrove, New England, New South Wales</i>	27
<i>Razorback Mine, Lachlan Fold Belt, New South Wales</i>	31
Chapter 4 Results	33
<i>A Possible New Stibiconite Group Mineral from Broken Hill, New South Wales</i>	33
<i>Other Mineral Syntheses</i>	34
<i>Solubility Studies</i>	36
<i>Mineral and Water Samples</i>	38
<i>Bayley Park Geochemical Orientation Survey</i>	41
Chapter 5 Discussion	42
<i>Solubility Phenomena</i>	42
<i>Secondary Mineral Assemblages</i>	44
<i>Bayley Park Geochemical Orientation Survey</i>	45
Concluding Comments	49
References	50
Appendix 1	57
<i>Microprobe data for the unnamed pyrochlore mineral from the Consols mine, Broken Hill</i>	
Appendix 2	59
<i>Bayley Park Soil Geochemistry Assays</i>	
Appendix 3	64
<i>Refinement Details for Unit Cell Data of Mineral Phases</i>	

ABSTRACT

An assessment of the secondary minerals of antimony (Sb) has been made in view of the role that they play in the dispersion of the element in aqueous solution in the vicinity of oxidising primary ores that carry Sb. Of the 40 or so secondary minerals known, only a few occur commonly. Chief among these are members of the stibiconite group, particularly stibiconite, $\text{SbSb}_2\text{O}_6\text{OH}$, bindheimite, $\text{Pb}_2\text{Sb}_2\text{O}_7$, and roméite, $\text{Ca}_2\text{Sb}_2\text{O}_7$; tripuhyite, FeSbO_4 , is also widespread in oxidised settings.

Previous workers have suggested that Sb is quite mobile in the supergene environment, but recently this has been challenged by others. The reason for the earlier conclusion can be traced to the assumption that $\text{Sb}_2\text{O}_5(\text{s})$ may be used as a proxy to describe the behaviour of Sb(V). This has been shown to be in error. Bindheimite, roméite and tripuhyite have been synthesised for the first time from aqueous solution and the solubilities of the former two have been measured in dilute 0.1 M aqueous HNO_3 . Total dissolved Sb at 25°C amounts to only a few ppb. In addition, the solubilities of the isomorphous minerals bottinoite, $\text{Ni}[\text{Sb}(\text{OH})_6]_2 \cdot 6\text{H}_2\text{O}$, and brandholzite, $\text{Mg}[\text{Sb}(\text{OH})_6]_2 \cdot 6\text{H}_2\text{O}$, have been measured in water at 25°C. These data have been used in turn to calculate their standard free energies of formation at this temperature and to comment on their modes of occurrence in natural settings. A synthesis of tripuhyite from aqueous solution has been developed as has a synthesis of a potentially new mineral, ideally $\text{Fe}_2\text{Sb}_2\text{O}_7$, from Broken Hill, New South Wales.

It has been shown conclusively that the cubic mineral pyrochlore $\text{Sb}_2\text{O}_5 \cdot 4\text{H}_2\text{O}(\text{s})$ and its cation-exchanged derivatives (stibiconite group minerals) control the solubility of Sb(V) in oxidised settings. It is concluded that Sb is in fact quite immobile under near surface conditions. This serves to limit the dispersion of the element in soil, surface and ground waters. The conclusion is reinforced by the characterisation of oxidised Sb mineral assemblages from several New South Wales deposits.

On the basis of the above findings, an orientation geochemical survey has been carried out over the Bayley Park Sb prospect near Hillgrove, New South Wales. Results from the chemical study have been validated, in that the extent of Sb dispersion in soils over the deposit is very limited. In addition, identification of secondary Sb minerals in very close association with oxidising stibnite, Sb_2S_3 , from several New South Wales deposits has

shown that the bulk of the secondary phases remain essentially *in situ*. This mirrors known occurrences world-wide.

The study has shown that soil sampling and analysis for Sb is highly effective as a guide to Sb ore deposits. This is of some use in exploration geochemical programs. On the other hand, Sb is almost certainly of no use as a pathfinder element in regional geochemical exploration, despite its extensive use as such in the past.

STATEMENT OF AUTHENTICATION

I, Glen Alfred Diemar, declare that this thesis contains no material that has been submitted for the award of any other degree or diploma and that, to the best of my knowledge, this thesis contains no material previously published or written by another person, except when due reference has been made in the text.

ACKNOWLEDGEMENTS

I would like to express my most sincere appreciation to Professor Peter Williams for his help and guidance throughout the course of the study. I feel honoured to be one of his “chemical children” and will strive to continue the legacy. I am also deeply indebted to Professor Peter Leverett for the time he devoted to my supervision, his willingness to share his knowledge, and his friendship.

Straits Hillgrove Gold Ltd is thanked for financial support and access to lease areas, geochemical and drill core data, all facilitated by Phil Shields. Chris Simpson provided field assistance and help with preparing several of the diagrams. Colin Dell and Scott Edwards also are gratefully acknowledged for their assistance in the field, sometimes under trying weather conditions. I thank them too for taking the time to help me and I know we will remain friends and colleagues long into the future.

My family and my soul mate Marta Sokolowski are especially thanked for their continuing support, encouragement and love throughout my university career.

The Australian Institute of Geoscientists (AIG) and the Sydney Mineral Exploration Discussion Group (SMEDG) are thanked for their financial support through the AIG-SMEDG student bursary program.

PUBLICATIONS IN SUPPORT OF THIS THESIS

Diemar, G.A., Filella, M., Leverett, P. and Williams, P.A. (2008) Dispersion of antimony from oxidizing ore deposits. *Pure and Applied Chemistry*, in press.

Diemar, G.A., Leverett, P. and Williams, P.A. (2008) Supergene dispersion of antimony and a geochemical exploration model for antimony ore deposits. *Proceedings PACRIM Congress Extended Abstracts Volume*. The Australasian Institute of Mining and Metallurgy, Melbourne, in press.

CHAPTER 1 INTRODUCTION

Antimony exists in oxidation states -III, 0, III and V, but is most commonly found in Nature in states III and V. Conflicting solubility and thermochemical data in the literature for Sb minerals have hampered our understanding of the chemical fate of Sb in oxidising Sb ore deposits. This has led to problems concerning Pourbaix diagrams with respect to just which species can be important in the natural environment.

Sulfide and sulfosalt minerals mostly form deep in the earth at high temperatures and under comparatively reducing conditions. They remain stable as long as they are protected from oxygen but, with few exceptions, sulfides and sulfosalts are intrinsically unstable above the water table and react with oxygen, resulting in higher oxidation states; notably, sulfide is ultimately transformed to sulfate. This general process has a very important consequence with respect to solubility phenomena (Williams, 1990). Sulfides and sulfosalts are extremely insoluble in water under ambient conditions. However, their oxidized equivalents are much more soluble and are transported in soil and ground water away from their original settings. For geochemical exploration, an understanding of the processes involved in such transport is vital for success and details of the geochemical behaviour of many elements in the supergene zone remain, at best, sketchy.

Attention in this thesis is focussed on the element antimony. A series of comprehensive reviews by Filella *et al.* (2002a,b), Filella and May (2003) has done much to increase our understanding of the behaviour of Sb in the natural environment, but the geochemistry of Sb in the vicinity of oxidising primary ores is still poorly understood. Several hundred primary Sb minerals are known (Anthony *et al.*, 1990-2003) and all are essentially insoluble in water under ambient conditions. It is the secondary phases formed under oxidizing conditions that act as metal ion buffers, and control the dispersion of Sb in surface and soil waters. Some 40 such minerals are known (Anthony *et al.*, 1990-2003); many are rare, but common species have become the focus of study in an effort to elucidate the geochemical behaviour of Sb in oxidised settings. This project reports studies of the solubilities of several common or geochemically significant Sb(V) minerals. The results indicate that Sb is much less mobile in the supergene zone than has previously been assumed. Implications for exploration geochemistry using Sb as a pathfinder element are discussed.

Secondary Antimony Minerals

The known secondary minerals of Sb are listed in Table 1.1. The number given after the mineral name refers to the number of localities in which they occur listed by www.mindat.org in July 2007. Stoichiometries indicated are based for the most part on single-crystal X-ray determinations (Anthony *et al.*, 1990-2003) and reference is made to these where appropriate or to other sources for more recent structure determinations, where appropriate.

The topographical listing in mindat.org is recognised as being imperfect and other localities for a number of the secondary minerals may be gleaned from the literature (*vide infra*). Nevertheless, the tabulation does indicate which phases are common and thus likely to be generally present in significant amounts in the oxidized zones of Sb-rich ore deposits. This has been used as a guide in the selection of species that should be incorporated in any supergene dispersion model for antimony. With a view towards a functional model for their influence on antimony dispersion in the regolith and natural waters, very rare species may be largely passed over because they almost certainly form under geochemical conditions that are rarely encountered. In this respect, they are geochemical and mineralogical ‘freaks’.

Table 1.1 indicates that only ten species are expected to commonly buffer Sb in natural aqueous solutions, leaving aside adsorption processes and interactions with dissolved organic matter. These common phases are simple oxides of Sb(III), a mixed Sb(III)-Sb(V) oxide, kermesite, tripuhyite, and members of the stibiconite group. Some of them are reported to occur in hundreds of deposits and it might be expected that as such all would be thoroughly characterized. Nevertheless, a number of ambiguities remain concerning structural and stoichiometric properties, and relative stabilities.

The stibiconite group comprises bismutostibiconite, bindheimite, partzite, roméite, stetefeldtite and stibiconite. Formulae given reflect, in part, solid solution phenomena (which are pervasive; see for example Vitaliano and Mason 1952; Mason and Vitaliano, 1953; Anthony *et al.*, 1990-2003; Brugger *et al.*, 1997), lattice vacancies inherent in the structures, and potential end-member compositions. The group is a sub-set of the pyrochlore family of general formula $A_{2-p}B_2X_{6-q}Y_{1-r} \cdot sH_2O$ that crystallizes in the cubic space group $Fd\bar{3}m$.

Table 1.1. The secondary Sb minerals.

Biehlite	1	$[(\text{Sb},\text{As})\text{O}]_2\text{MoO}_4$
Bindheimite	314	$\text{Pb}_2\text{Sb}_2\text{O}_6(\text{O},\text{OH})$
Bismutostibiconite	6	$\text{Bi}(\text{Sb},\text{Fe})_2\text{O}_7$
Bottinoite	11	$\text{Ni}[\text{Sb}(\text{OH})_6]_2 \cdot 6\text{H}_2\text{O}$
Brandholzite	3	$\text{Mg}[\text{Sb}(\text{OH})_6]_2 \cdot 6\text{H}_2\text{O}$
Brizzite	1	NaSbO_3
Byströmite	2	MgSb_2O_6
Camerolaite	1	$\text{Cu}_4\text{Al}_2(\text{HSbO}_4,\text{SO}_4)\text{CO}_3(\text{OH})_{10} \cdot 2\text{H}_2\text{O}$
Cervantite	185	Sb_2O_4
Cetineite	6	$(\text{K},\text{Na})_6(\text{Sb}_2\text{O}_3)_6(\text{SbS}_3)_2[(\text{H}_2\text{O})_{6-x}(\text{OH})_x]$ ($x = 0.5$)
Clinocervantite	2	Sb_2O_4
Coquandite	5	$\text{Sb}_6\text{O}_8\text{SO}_4 \cdot \text{H}_2\text{O}$
Cualstibite	3	$\text{Cu}_2\text{Al}[\text{Sb}(\text{OH})_6](\text{OH})_6$
Cyanophyllite	7	$(\text{Cu},\text{Al})_3(\text{OH})_6[\text{Sb}(\text{OH})_6]$ ($\text{Cu}:\text{Al} \approx 2.7:1$)
Kelyanite	1	$\text{Hg}_{12}\text{Sb}(\text{Cl},\text{Br})_3\text{O}_6$
Kermesite	161	$\text{Sb}_2\text{S}_2\text{O}$
Kleibelsbergite	8	$\text{Sb}_4\text{O}_4\text{SO}_4(\text{OH})_2$
Mallestigitite	2	$\text{Pb}_3\text{Sb}(\text{SO}_4)(\text{AsO}_4)(\text{OH})_6 \cdot 3\text{H}_2\text{O}$
Mammothite	4	$\text{Pb}_6\text{Cu}_4\text{AlSbO}_2(\text{SO}_4)_2\text{Cl}_4(\text{OH})_{16}$
Mopungite	6	$\text{NaSb}(\text{OH})_6$
Nadorite	13	PbSbO_2Cl
Onoratoite	2	$\text{Sb}_8\text{O}_{11}\text{Cl}_2$
Ottensite	1	$(\text{Na},\text{K})_3(\text{Sb}_2\text{O}_3)_3(\text{SbS}_3) \cdot 3\text{H}_2\text{O}$
Partzite	36	$\text{Cu}_2\text{Sb}_2(\text{O},\text{OH})_7$
Peretaite	3	$\text{CaSb}_4\text{O}_4(\text{SO}_4)_2(\text{OH})_2 \cdot 2\text{H}_2\text{O}$
Richelsdorfite	31	$\text{Ca}_2\text{Cu}_5[\text{Sb}(\text{OH})_6](\text{AsO}_4)_4\text{Cl} \cdot 6\text{H}_2\text{O}$
Roméite	32	$(\text{Ca},\text{Fe},\text{Mn},\text{Na})_2(\text{Sb},\text{Ti})_2\text{O}_6(\text{O},\text{OH},\text{F})$
Rosiaite	6	PbSb_2O_6
Sabelliite	3	$\text{Cu}_2\text{Zn}(\text{AsO}_4,\text{SbO}_4)(\text{OH})_3$
Schafarzikite	8	FeSb_2O_4
Sénarmontite	124	Sb_2O_3
Shakhovite	6	$\text{Hg}_4\text{SbO}_3(\text{OH})_3$
Stetefeldtite	23	$\text{Ag}_2\text{Sb}_2(\text{O},\text{OH})_7$
Stibiconite	275	$\text{SbSb}_2\text{O}_6(\text{OH})$
Theisite	27	$\text{Cu}_5\text{Zn}_5(\text{AsO}_4,\text{SbO}_4)_2(\text{OH})_{14}$
Thorikosite	3	$\text{Pb}_3(\text{Sb},\text{As})\text{O}_3(\text{OH})\text{Cl}_2$
Tripuhyite	40	FeSbO_4
Valentinite	231	Sb_2O_3
Zincalstibite	1	$\text{Zn}_2\text{Al}[\text{Sb}(\text{OH})_6](\text{OH})_6$

In the lattice (Figure 1.1) *A* ions occupy $16d$ ($\frac{1}{2}, \frac{1}{2}, \frac{1}{2}$) and *B* ions $16c$ (0,0,0). Oxide, hydroxide or fluoride ions occupy the *X* ($48f$; $x, \frac{1}{8}, \frac{1}{8}$) and *Y* ($8b$; $\frac{3}{8}, \frac{3}{8}, \frac{3}{8}$) sites, respectively, and water molecules can substitute at both *A* and *Y* positions. An extraordinary flexibility in terms of its ability to accommodate a range of different cations is a feature of the lattice, as is its ability to tolerate vacancies. Thus $0 \leq p \leq 2$, $0 \leq r \leq 1$ and $s < 2$. Normally $q = 0$, but some limited vacancy can occur on this site (Lumpkin and Ewing, 1992). As far as the stibiconite group is concerned, some structures have long been established (Zedlitz, 1932;

Natta and Baccaredda, 1933) and some species erroneously described as Sb_2O_4 , Sb_2O_5 , or $\text{Sb}_2\text{O}_5 \cdot n\text{H}_2\text{O}$ (Dehlinger, 1928). Dihlstrom and Westgren (1937) pointed out that a product of heating $\text{Sb}(\text{OH})_5$ was identical to compounds studied by Natta and Baccaredda, Dehlinger, and Dehlinger and Glocker (1927), and that it was in fact cubic $\text{Sb}_3\text{O}_6\text{OH}$, space group $Fd\bar{3}m$, with 8 Sb atoms statistically distributed over the A sites. Ideal, end-member stibiconite had $a = 10.28 \text{ \AA}$. Gasperin (1955) confirmed the above conclusions concerning synthetic $\text{Pb}_2\text{Sb}_2\text{O}_7$ and the crystal chemistry of roméite has been reviewed more recently (Brugger *et al.*, 1997). Brisse *et al.* (1972) have also published solid state synthetic routes to *inter alia*, $\text{Ca}_2\text{Sb}_2\text{O}_7$ and $\text{Pb}_2\text{Sb}_2\text{O}_7$. The single-crystal X-ray structure of “lewisite” (= roméite) was more recently reported, confirming the conclusions of earlier workers (Zubkova, *et al.*, 2000).

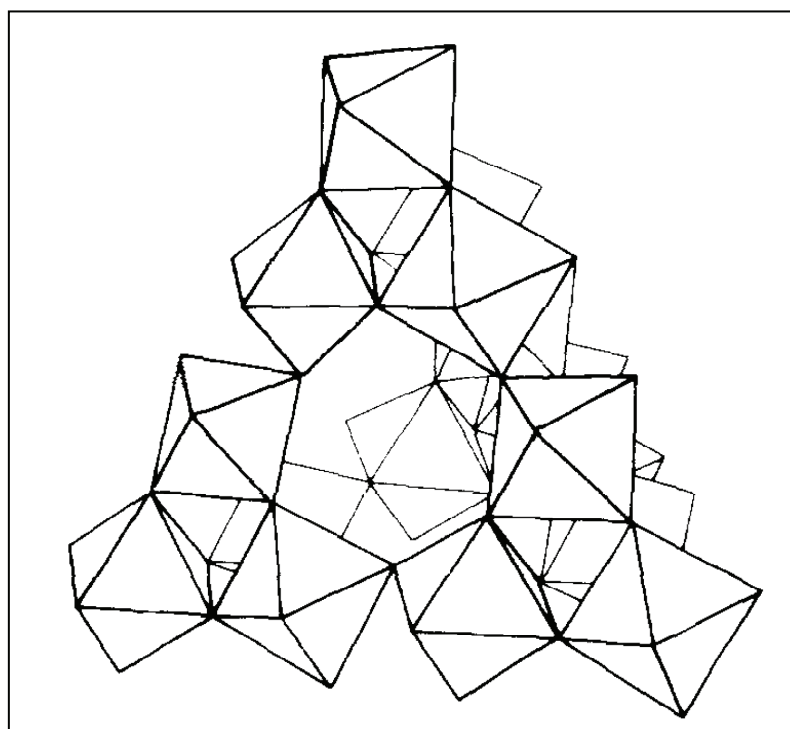


Figure 1.1. The cubic $A_{2-p}B_2X_{6-q}Y_{1-r} \cdot s\text{H}_2\text{O}$ or $A_2B_2O_6(\text{O},\text{OH})$ pyrochlore framework (England *et al.*, 1980); cations and water molecules are accommodated in the large voids surrounded by SbO_6 octahedra.

The nature of the mineral stetefeldtite, nominally $\text{Ag}_2\text{Sb}_2(\text{O},\text{OH})_7$, rests on the work of Mason and Vitaliano (1953). Powder X-ray data were analogous to those of bindheimite and gave the pyrochlore pattern with $a = 10.46 \text{ \AA}$. Inclusion of the mineral in the stibiconite group has been corroborated in a series of synthetic studies. Schrewelius (1938) synthesized the pyrochlore $\text{Ag}_2\text{Sb}_2\text{O}_6$ and found $a = 10.25 \text{ \AA}$; Sleight (1969) found $a = 10.249 \pm 0.002 \text{ \AA}$ for the same phase. A more exhaustive study by Stewart and Knop

(1970) revealed a range of stoichiometries that could be achieved for the Ag antimonate. Solid state syntheses yielded $\text{Ag}_{0.97}\text{Sb}^{\text{III}}_{0.79}\text{Sb}^{\text{V}}_{2.13}\text{O}_7$, $\text{Ag}_{1.36}\text{Sb}^{\text{III}}_{0.49}\text{Sb}^{\text{V}}_{2.23}\text{O}_7$, $\text{Ag}_{1.77}\text{Sb}^{\text{III}}_{0.94}\text{Sb}^{\text{V}}_{2.13}\text{O}_7$, $\text{Ag}_{2.43}\text{Sb}^{\text{III}}_{0.29}\text{Sb}^{\text{V}}_{2.14}\text{O}_7$ and $\text{Ag}_2\text{Sb}_2\text{O}_6$, depending on the reagents and mol ratios employed. Precipitation from aqueous solutions of AgNO_3 and $\text{KSb}(\text{OH})_6$ of varying concentrations and pH values, followed by firing at 500-700°C, gave $\text{AgSb}_3\text{O}_{7.3}$, $\text{AgSb}_3\text{O}_{7.1}$, $\text{AgSb}_3\text{O}_{6.9}$ and $\text{Ag}_2\text{Sb}_2\text{O}_6$. All had the pyrochlore structure with a ranging from 10.249 to 10.296 ± 0.001 Å. Walenta (1983) showed bismutostibiconite to be cubic, space group $Fd\bar{3}m$, $a = 10.384$ Å; a Bi-rich bindheimite from Namibia had previously been described (Bothwell *et al.*, 1960)

The final member of the stibiconite group, partzite, is more problematic. Its formula is questionably quoted as $\text{Cu}_2\text{Sb}_2(\text{O},\text{OH})_7$, ideally $\text{Cu}_2\text{Sb}_2\text{O}_7$, and has been reported from some 36 localities. Although the mineral was originally described nearly 150 years ago (Arents, 1867), accepted characteristic data for the mineral again depend upon the careful work of Mason and Vitaliano (1953). These workers note that others had discounted the mineral as a mixture of several phases, and samples of which contained no detectable Sb (Ransome, 1940). In this connection Dunning and Cooper (2005) found dark green veins of partzite in massive tetrahedrite at the Murdock mine, Plumas County, California. Other massive green material after tetrahedrite was shown to consist of stibiconite impregnated by tiny malachite grains.

Nevertheless, several specimens from the type locality were examined by Mason and Vitaliano (1953) and found spectrographically to contain dominant Cu and Sb. Powder X-ray measurements gave an indexed diffraction pattern for a pyrochlore structure with $a = 10.25$ Å, but the analysis was not considered to be reliable. The situation is rather more confused by reports of a substance named “protopartzite” from Veitsch, Austria, one of the localities noted for partzite (Koritnig, 1967). Electron microprobe analyses with water by difference led to a formula of $\text{Cu}(\text{Sb},\text{As},\text{Fe},\text{Zn})_{1.3}(\text{O},\text{OH})_{6.8}$ but the material was X-ray amorphous and the name has not been accepted as a mineral by the International Mineralogical Association. Even more puzzling is a more recent report (Ertl and Brandstätter, 2000) of an earthy, olive green alteration product of tetrahedrite from the same locality. This had the cubic pyrochlore structure with $a = 10.295(10)$ Å and an analysis indicated a formula of $(\text{Cu},\text{As},\text{Fe},\text{Zn})_2(\text{Sb},\text{Fe})_2\text{O}_6(\text{O},\text{OH},\text{F})$. Among the known Cu(II)-Sb(V) oxides are CuSb_2O_6 and $\text{Cu}_9\text{Sb}_4\text{O}_{19}$. The former has been known for some time (Byström *et al.*, 1941), and its structure determined by Rietvelt analysis of neutron

powder diffraction data (Nakua *et al.*, 1991). $\text{Cu}_9\text{Sb}_4\text{O}_{19}$ has a body-centred cubic structure with $a = 9.620 \text{ \AA}$ (Shimada *et al.*, 1985; Shimada and Ishii, 1989). In addition, the Cu(I) species $\text{Cu}_8\text{Sb}_2\text{O}_9$ is known and a poorly-described lower symmetry polymorph of $\text{Cu}_8\text{Sb}_2\text{O}_9$ has been synthesized (Shimada and Mackenzie, 1982; Shimada *et al.*, 1988). Furthermore, two mixed oxidation state species Cu_5SbO_6 and $\text{Cu}_2\text{SbO}_{5.75}$ have been reported (Kol'tsova and Chastukhin, 2002). It therefore seems probable that partzite (*sensu stricto*) does not exist.

By comparison, the chemistry of the remaining commonly found secondary Sb minerals is quite straightforward. Kermesite, $\text{Sb}_2\text{S}_2\text{O}$, is an intermediate in the oxidation of stibnite to other oxides and is frequently associated with s enarmontite, valentinite, cervantite and stibiconite (Anthony *et al.*, 1990-2003). Its structure was originally reported by Kupcik (1967) and later refined by Bonazzi *et al.* (1987). Four simple secondary oxides are known, clinocervantite, cervantite, and the dimorphs of composition Sb_2O_3 , s enarmontite and valentinite. Clinocervantite is known only from two deposits (Basso *et al.*, 1999), but cervantite, $\alpha\text{-Sb}_2\text{O}_4$, s enarmontite and valentinite are known to occur in hundreds of localities, usually in combination and often as the result of oxidation of stibnite (Anthony *et al.*, 1990-2003; Table 1.1). Sb_2O_5 is not known as a mineral, but is known as two synthetic phases (Jansen, 1979a,b), as is the hydrated Sb(V) oxide, $\text{Sb}_5\text{O}_{12}(\text{OH})\cdot\text{H}_2\text{O}$ (Jansen, 1978); another mixed valence state oxide, $\text{Sb}_6\text{O}_{13} = \text{Sb}_2\text{O}_3\cdot 2\text{Sb}_2\text{O}_5$, is known synthetically (Massalski, 1990). However, a number of naturally occurring species possess stoichiometries based on salts of $\text{Sb}(\text{OH})_6^-$. A third high-temperature polymorph of Sb_2O_3 is known (Orosel, 2007), but has not been reported to occur naturally.

An Fe-Sb oxide, tripuhyite, is worthy of comment. It was first described more than a century ago from alluvial deposits in Brazil (Hussak and Prior, 1897). Although its exact composition remained in doubt for some time, Mason and Vitaliano (1953) correctly concluded that its formula was FeSbO_4 and this has been recently proven beyond doubt. (Berlepsch *et al.*, 2003; Basso *et al.*, 2003). Tripuhyite has been reported from some forty localities. In the majority of cases it is observed as an alteration product of stibnite and other Fe-bearing sulfides. Less commonly it is seen as an alteration product of the tetrahedrite-tennantite series.

Richelsdorfite, cyanophyllite, mallestigte, cualstibite, and zincalstibite all contain the $\text{Sb}(\text{OH})_6^-$ ion, as do brandholzite, $\text{Mg}[\text{Sb}(\text{OH})_6]_2 \cdot 6\text{H}_2\text{O}$, bottinoite, $\text{Ni}[\text{Sb}(\text{OH})_6]_2 \cdot 6\text{H}_2\text{O}$, and mopungite, $\text{NaSb}(\text{OH})_6$. The latter three are known synthetic compounds and have been structurally characterised (Jander and Brüll, 1926; Beintema, 1936; Williams, 1985; Bonazzi *et al.*, 1992; Friedrich *et al.*, 2000, 2003; Palenik *et al.*, 2005). Brandholzite is a rare secondary mineral, and mopungite is nearly as rare. Some 11 localities are known for bottinoite, which was originally reported, not surprisingly, as an alteration product of ullmannite, NiSbS (Bonazzi *et al.*, 1992). This association is mirrored elsewhere and it is remarkable that ullmannite is present in every deposit that hosts bottinoite in the oxidized zone (Anon., 1988; Weiss, 1990; Pawlowski, 1991; Clark, 1993; Green *et al.*, 2000; Wittern, 2001; Viñals and Calvo, 2006; Berbain and Favreau, 2007; mindat.org). Nine of the localities carry millerite, NiS , or other Ni-bearing sulfosalts.

Simple Aqueous Antimony Chemistry

Pourbaix Diagrams

Previous attempts to describe the basic geochemical behaviour of Sb have adopted the classical Pourbaix diagram approach. The first such report was published more than 50 years ago (Pitman *et al.*, 1957) and subsequent modifications have attempted to refine Pourbaix's original description (Brookins, 1986; Vink, 1996). All of these descriptions have suffered from a lack of reliable values for the thermochemical properties of many of the species that were incorporated in calculations. In particular, reliable values of $\Delta_f G^\circ$ for cervantite, Sb_2O_4 , sénarmontite and valentinite, dimorphs of composition Sb_2O_3 were either not available or overlooked. Fortunately, this deficiency has now been rectified (Pankajavalli and Sreedharan, 1987; Zotov *et al.*, 2003) and the most reliable values for the simple oxide minerals of Sb(III,V) are listed in Table 1.2, together with data for a selected number of other solid phases. An enduring problem, however, concerns the fact that the geochemical behaviour of Sb under oxidizing conditions has been interpreted on the basis of the solubility of $\text{Sb}_2\text{O}_5(\text{s})$. Baes and Mesmer (1976) derived a value for $\lg K_{\text{S}10}$ of -3.7 at 25°C , based on earlier solubility studies (Tourky and Mousa, 1948). Later workers reported solubility data for Sb_2O_5 that were consistent with the above value (Jain and Banerjee, 1961; Casas *et al.*, 2004). This, coupled with a value for $\Delta_f G^\circ(\text{Sb}_2\text{O}_{5,\text{s}}, 298.15\text{K})$ (Wagman *et al.*, 1982), allowed Sb to be thought to be easily dispersed in the natural environment. Thus Vink (1996) noted the "...relatively high mobility of antimony under oxidizing conditions be it acidic or alkaline", a remark echoed elsewhere in that Sb is "...relatively

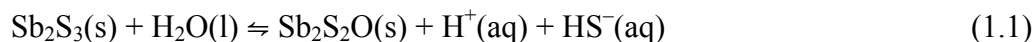
mobile in the environment, especially under oxic conditions” (Krupka and Serne. 2002). Other comments on the matter have been more cautious or contradictory. Filella *et al.* (2002a) suggested that “...little is known about the environmental mobility of antimony...”; Wilson *et al.* (2004), in a study of a contaminated smelter site, concluded that “...antimony is not readily mobilised into the environment...”.

For simplicity the oxidation of stibnite is the focus here as it is the most common primary Sb-bearing phase aside from members of the tetrahedrite group. Apparently reliable ΔfG° data at 298.15K are available for stibnite, Sb_2S_3 (Bryndzia and Kleppa, 1988; Seal *et al.*, 1992).

Table 1.2. Most reliable thermodynamic data for simple antimony minerals and related phases (T = 298.15 K).

		$\Delta fG^\circ/kJ\ mol^{-1}$	Reference
Stibnite	$Sb_2S_3(s)$	-149.9 ± 2.1	Bryndzia and Kleppa (1988); Seal <i>et al.</i> (1992)
Kermesite	$Sb_2S_2O(s)$	-406.5	Williams-Jones and Normand (1997) Babčan (1976); see text
Sénarmontite	$Sb_2O_3(s)$	-633.2 ± 2.1	Zotov <i>et al.</i> (2003)
Valentinite	$Sb_2O_3(s)$	-625.9 ± 2.1	Zotov <i>et al.</i> (2003)
Cervantite	$Sb_2O_4(s)$	-754.5 ± 1.6	Pankajavalli and Sreedharan (1987)
	$Ca[Sb(OH)_6]_2(s)$	-3061.6	Johnson <i>et al.</i> (2005); see text
	$Sb_2O_5(s)$	-829.3	Wagman <i>et al.</i> (1982)
Mopungite	$Na[Sb(OH)_6](s)$	-1508.5	Blandamer <i>et al.</i> (1974); see text

The least oxidized product of stibnite is kermesite, Sb_2S_2O . Williams-Jones and Normand (1997) derived the relationship $\lg K = 4126.5/T(K) - 18.278$ for equation (1.1), based on the work of Babčan (1976).



From this $\Delta fG^\circ(Sb_2S_2O,s,298.15K)$ is derived as $-406.5\ kJ\ mol^{-1}$ using the ΔfG° value for stibnite above and values for H_2O and ionic species given listed by Robie and Hemingway (1995). Under increasingly oxidizing conditions sénarmontite or valentinite, Sb_2O_3 , is formed, followed in turn by cervantite, Sb_2O_4 , stibiconite, Sb_3O_6OH , and other members of the stibiconite group devoid of Sb(III). For some time the value $\Delta fG^\circ(298.15K)$ for valentinite of $-626.4 \pm 3.0\ kJ\ mol^{-1}$ was accepted as being the most accurate Wagman *et al.* (1982) and this may be compared quite favourably with the more recent results of Zotov *et al.* (2003); the latter workers derived $\Delta fG^\circ(Sb_2O_3,s, valentinite,298.15K) = -625.9 \pm 2.1$

kJ mol^{-1} and $\Delta fG^\circ(\text{Sb}_2\text{O}_3, \text{s}, \text{sénarmontite}, 298.15\text{K}) = -633.2 \pm 2.1 \text{ kJ mol}^{-1}$ and these values are adopted here. The generally accepted value for $\Delta fG^\circ(\text{Sb}_2\text{O}_4, \text{s}, \text{cervantite}, 298.15\text{K})$ is $-795.8 \text{ kJ mol}^{-1}$ (Wagman *et al.*, 1982), but a range of values is found in the literature. Published solubilities of cervantite (Konopik and Zwiauer, 1952) are consistent with the value obtained from Pankajavalli and Sreedharan (1987), but not that of Wagman *et al.* (1982) and it is apparent that the $\Delta fG^\circ(\text{Sb}_2\text{O}_4, \text{s}, \text{cervantite})$ value derived from Pankajavalli and Sreedharan (1987) must be the more accurate.

Unfortunately there are no thermodynamic quantities available in the literature for members of the stibiconite group. Swaminathan and Sreedharan (2003) reported electrochemical measurements of tripuhyite, FeSbO_4 , and schafarzikite, FeSb_2O_4 , at temperatures from 771–981 K and found the relationships $\Delta fG^\circ(\text{FeSbO}_4, \text{s}) = -976.9 + 0.3289T \text{ (K)} \pm 5.5 \text{ kJ mol}^{-1}$ and $\Delta fG^\circ(\text{FeSb}_2\text{O}_4, \text{s}) = -1068.7 + 0.3561T \text{ (K)} \pm 3.5 \text{ kJ mol}^{-1}$. This leads to values of ΔfG° for tripuhyite and schafarzikite of -878.8 ± 5.5 and $-962.5 \pm 3.5 \text{ kJ mol}^{-1}$, respectively, at 298.15 K. It is regrettable that the extrapolation to 298.15 K is not sufficiently reliable for these findings to be applied at ambient temperatures.

Solubility data from 25 to 55°C for $\text{Na}[\text{Sb}(\text{OH})_6]$ have been reported (Blandamer *et al.*, 1974) and from these it is possible to estimate ΔfG° of mopungite at 298.15 K (see Experimental section). Johnson *et al.* (2005) reported unpublished values for the solubility products at (presumably) 25°C of $\text{Ca}[\text{Sb}(\text{OH})_6]_2(\text{s})$ and $\text{Pb}[\text{Sb}(\text{OH})_6]_2(\text{s})$ of $10^{-12.55}$ and $10^{-11.02}$, respectively. Neither is as yet known as a naturally occurring mineral but it is worth noting that the magnitudes of the solubility products indicate that Ca^{2+} and Pb^{2+} are somewhat more effective than Na^+ in reducing the solubility of Sb(V) in aqueous solution. Work undertaken during the course of this study indicates that the compounds Johnson *et al.* studied are in fact metastable (see below). A Pourbaix diagram using the currently most reliable thermochemical data for simple Sb oxide phases and $\text{Ca}[\text{Sb}(\text{OH})_6]_2$ is shown in Figure 1.2. It must however be noted that the field occupied by $\text{Ca}[\text{Sb}(\text{OH})_6]_2$ (“ CaSb_2O_6 ”) refers to an amorphous material (see below).

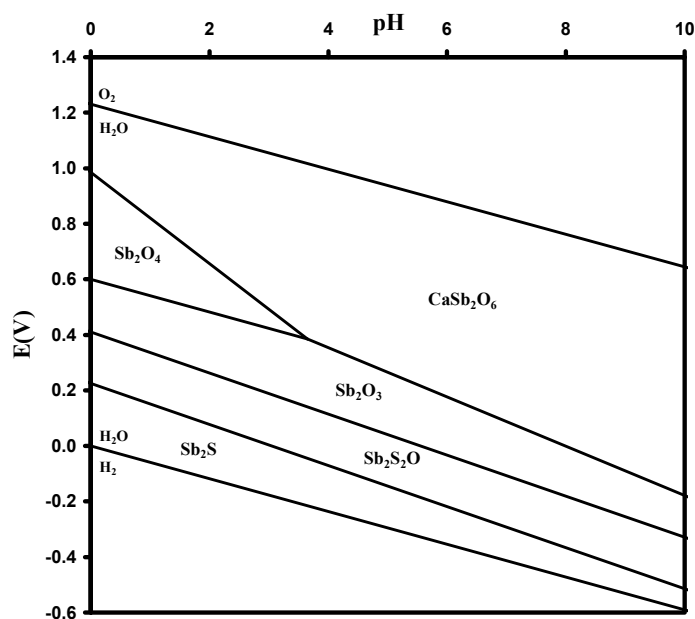


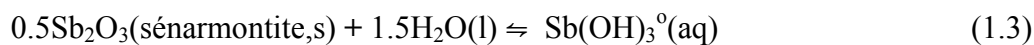
Figure 1.2. Pourbaix diagram for simple Sb mineral phases.

Aqueous Species and Hydrolysis of Sb(III) and Sb(V)

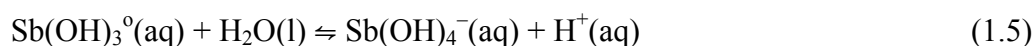
In order to properly account for solubilities of salts reported in the present study, it is essential to have an understanding of the hydrolysis and extent of complexation of Sb(III) and, especially, Sb(V) in aqueous solution. As it transpires, the chemistry of Sb in both oxidation states is remarkably simple with respect to ligands of geochemical significance.

Baes and Mesmer (1976) summarised available data, pointing out that the solubility of $\text{Sb}_2\text{O}_3(\text{s})$ can be adequately accounted for by the three species $\text{Sb}(\text{OH})_2^+(\text{aq})$, $\text{Sb}(\text{OH})_3^0(\text{aq})$ and $\text{Sb}(\text{OH})_4^-(\text{aq})$ over the pH range from 0 to 14. It was also noted that less hydrolysed species could only exist in very concentrated acid solutions and that polymer formation is insignificant at Sb(III) concentrations less than 0.1 M. Data reported subsequently are in excellent agreement with that of earlier workers. The solubility of orthorhombic $\text{Sb}_2\text{O}_3(\text{s})$, equation (1.2), at 298.15 K was reported by Gayer and Garrett (1952) with $\lg K = -4.28 \pm 0.08$. Solubility data for equation (1.2) spanning the range $278 \leq T/\text{K} \leq 398$ (Schulze, 1883; Gayer and Garrett, 1952; Zotov *et al.*, 2003) give a satisfactory Arrhenius plot and the value of Gayer and Garrett (1952) is adopted here. Cubic $\text{Sb}_2\text{O}_3(\text{s})$ is the thermodynamically stable phase and Zotov *et al.* (2003) derived the relationship $\lg K = -2165.7/T(\text{K}) + 2.28$ for equation (1.3) over the range $378 \leq T/\text{K} \leq 698$ from solubility data.

Extrapolation to 298.15 K gives $\lg K = -4.98$.



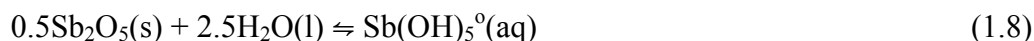
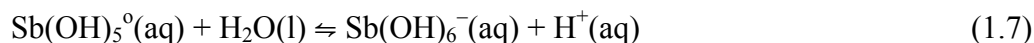
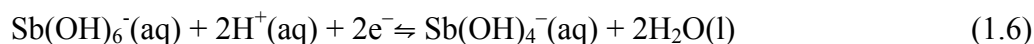
A reliable value for $\Delta\text{fG}^\circ(\text{Sb}(\text{OH})_3^\circ, \text{aq}, 298.15\text{K})$ of $-644.4 \pm 1.1 \text{ kJ mol}^{-1}$ is available, based on the careful solubility work of Zotov *et al.* (2003). Baes and Mesmer (1976) used the solubility data of Gayer and Garrett (1952) and Mishra and Gupta (1968) to calculate equilibrium constants for equations (1.4) and (1.5) noting that the value for the former was consistent with the work of Schuhmann (1924). However, Mishra and Gupta (1968) conducted their experiments at 23°C.



Values of $\lg K$ at 298.15 K for (1.4) and (1.5) are 1.41 and -11.82 , respectively. Filella and May (2003) used the Jess strategy to calculate corresponding values of -1.371 and -11.70 in good agreement with the above (note that there is an apparent sign error in their paper for the former). A recent experimental study by Zakaznova-Herzog and Seward (2006) confirmed the above values with $\lg K$ at 298.15 K for (1.4) and (1.5) being 1.38 ± 0.01 and -11.82 ± 0.02 , respectively, and these values are adopted here in subsequent calculations. Equations (1.4) and (1.5) can be combined with $\Delta\text{fG}^\circ(\text{Sb}(\text{OH})_3^\circ, \text{aq}, 298.15\text{K})$ to give $\Delta\text{fG}^\circ(298.15\text{K})$ values for the species $\text{Sb}(\text{OH})_2^+(\text{aq})$ and $\text{Sb}(\text{OH})_4^-(\text{aq})$ of -415.2 and $-814.0 \text{ kJ mol}^{-1}$, respectively.

Past (1985) reported $E^\circ = +0.363 \text{ V}$ at 298.15 K for the reaction given in (1.6), based on electrochemical measurements in aqueous KOH solutions reported by Grube and Schweigardt (1923). From the data above, $\Delta\text{fG}^\circ(\text{Sb}(\text{OH})_6^-, \text{aq}, 298.15\text{K})$ is found to be $-1218.2 \text{ kJ mol}^{-1}$. Lefebvre and Maria (1963) reported an experimental study of the hydrolysis of Sb(V) and Baes and Mesmer (1976) recalculated their data to yield a value of $\lg K(298.15\text{K}) = -2.72$ for equation (1.7); a more recent exhaustive study by Accornero *et al.* (2008) is in agreement, within experimental error. A value of $\Delta\text{fG}^\circ(\text{Sb}(\text{OH})_5^\circ, \text{aq}, 298.15\text{K}) = -996.6 \text{ kJ mol}^{-1}$ can be derived from the above data. The

best available value for $\Delta fG^{\circ}(\text{Sb}_2\text{O}_5, \text{s}, 298.15\text{K})$ is $-829.3 \text{ kJ mol}^{-1}$ (Wagman *et al.*, 1982) and this may be combined to give $\lg K = -1.89$ for equation (1.8). Thus at 298.15 K $\alpha(\text{Sb}(\text{OH})_5^{\circ}) = 10^{-1.89}$ and, for $\gamma(\text{Sb}(\text{OH})_5^{\circ}) = 1$, $[\text{Sb}(\text{OH})_5^{\circ}] = 0.013 \text{ m}$.

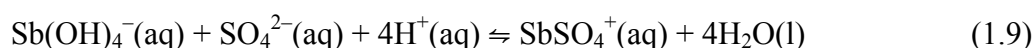


This derivation, based solely on accepted values of thermodynamic quantities and, as far as can be ascertained, reliable stability constant data, is noteworthy in several ways. First, it is comparable with the value for $\lg K_{\text{S}10}$ of -3.7 calculated by Baes and Mesmer (1976) using data for the solubility of $\text{Sb}_2\text{O}_5(\text{s})$ at 35°C in dilute acid (experiments involved $0.05\text{--}4.6 \text{ M}$ HCl) reported by Tourky and Mousa (1948). This value has been the only one quoted for such calculations since it was first published. Secondly, the value is remarkably, but fortuitously, close to that reported by Jain and Banerjee (1961), who prepared $\text{HSb}(\text{OH})_6$ using ion exchange methods and obtained a 0.0127 M solution with a pH of 2.6 at room temperature. Recently, another report of the solubility of $\text{Sb}_2\text{O}_5(\text{s})$ in aqueous H_2SO_4 at $298 \pm 0.2 \text{ K}$ has appeared (Casas *et al.*, 2004). At low acid concentrations ($0.001\text{--}0.102 \text{ m}$) experimental data are of rather low precision and give an average solubility of $1.17 \times 10^{-3} \text{ m}$ (Sb_2O_5), in reasonable agreement with the above. With increasing acid concentration solubility increased to $4.01 \times 10^{-3} \text{ m}$ at 8.707 m H_2SO_4 . Nevertheless, as is shown below, the systems studied are metastable with respect to hydrated antimonous acid.

As indicated by Baes and Mesmer (1976) the hydrolysis of $\text{Sb}(\text{V})$ in dilute solution is adequately accounted for by the two species $\text{Sb}(\text{OH})_5^{\circ}(\text{aq})$ and $\text{Sb}(\text{OH})_6^{-}(\text{aq})$ over the entire pH range normally encountered in geochemical systems. The literature is completely silent with respect to complex formation between $\text{Sb}(\text{OH})_4^{-}(\text{aq})$ or $\text{Sb}(\text{OH})_6^{-}(\text{aq})$ and metal ions in aqueous solution.

Complex Formation with Geochemically Common Inorganic Ligands

A review of the literature reveals that no complexes of geochemical significance other than hydrolysed species are important except under very acidic conditions. Stability constant data for these species are incomplete, but enough can be gleaned to take them into account for solution modelling purposes, in particular those involving sulfate and chloride. Nishimura and Tozawa (1986) first drew attention to the possibility of sulfate complexes of Sb(III) in sulfuric acid solutions. In a recent study of solubility in aqueous sulfuric acid at 25°C, Casas *et al.* (2004) found that the solubility of Sb₂O₃ could only be adequately explained when SbSO₄⁺(aq) was incorporated in the speciation scheme. A value for the equilibrium constant for equation (1.9) was derived as $\lg K = 22 \pm 1$ at 298 ± 0.2 K, based on the earlier work of Ryzhenko *et al.* (1985) and Kang *et al.* (1992).



The significance of the species SbSO₄⁺(aq) in supergene systems at ambient temperatures was assessed on the basis of the control of Sb dissolution by sénarmontite or valentinite, for which $[\text{Sb(OH)}_3^0] \approx 10^{-4}$ m. Speciation calculations concerning hydrolysed Sb(III) species, SbSO₄⁺(aq) and HSO₄⁻(aq) were performed for $[\text{SO}_4^{2-}]_{\text{tot}} = 0.01, 0.1$ and 1 m using COMICS (Perrin and Sayce, 1967; Lancashire, 1995). Under these conditions SbSO₄⁺(aq) is a significant species with respect to Sb(OH)₃⁰(aq) only at pH values less than about 4, 3 and 2, respectively. Casas *et al.* (2004) did not find any such evidence for complex formation between sulfate and Sb(V) in sulfuric acid solutions studied under the same conditions. Thus it is concluded that even under acidic conditions hydrolysed complexes of Sb(V) dominate its speciation. The rare secondary sulfate minerals coquandite, Sb₆O₈SO₄·H₂O and klebelsbergite, Sb₄O₄SO₄(OH)₂ (and perhaps other sulfates listed in Table 1) probably form under acidic conditions with high sulfate activities, when sulfate complexation can be important. Indeed, synthetic klebelsbergite was obtained by boiling Sb₂O₃ with sulfuric acid (Nakai and Appleman, 1980).

Complex formation between chloride ions, Sb(III) and Sb(V) in aqueous solution at ambient temperatures has been thoroughly reviewed by Filella and May (2003). Earliest available data for Sb(III) come from the work of Pantani and Desideri (1959), and for Sb(V) from Neumann (1954). Chloroantimonate(III) complexes are not highly stable although species in aqueous solution of composition SbCl_x^{3-x} with $1 \leq x \leq 6$ have been

reported. Equilibrium constants have been for the most part measured at high ionic strengths and under very acidic conditions. For this reason, Filella and May (2003) could not reliably re-interpret the data for higher homologues, although a satisfactory and internally consistent data set for $1 \leq x \leq 4$ was obtained. As far as the present study is concerned this presents no difficulty as salinities in hyper-acidic supergene aqueous systems do not reach levels that would stabilise complexes such as $\text{SbCl}_5^{2-}(\text{aq})$ or $\text{SbCl}_6^{3-}(\text{aq})$; hyper-acidity in these environments is invariably associated with sulfate-rich systems (Williams, 1990). Speciation calculations for complexes with $1 \leq x \leq 4$ and hydrolysed Sb(III) species were carried out as described above for sulfate at $1 \leq \text{pH} \leq 7$ for $[\text{Cl}^-]_{\text{tot}}$ up to 0.5 *m*. The chloride complexes are significant only at higher chloride concentrations and at $\text{pH} \leq 2$; at $[\text{Cl}^-]_{\text{tot}} = 10^{-3}$ *m* (ca 35 ppm) chloride complexes only account for approximately 0.002% of total dissolved Sb(III) even at a pH of 0. Another attempt to calculate a self-consistent set of stability constants for SbCl_x^{3-x} with $1 \leq x \leq 4$ was reported earlier by Belevantsev *et al.* (1998), who derived constants of between 2 and 6 orders of magnitude less than Filella and May (2003). Despite the wide variations for stability constants in the literature, the values derived by Belevantsev *et al.* (1998) predict even lower contributions to dissolved Sb concentrations at ambient temperatures in the supergene setting.

It may be considered that mixed chloro-hydroxo- species could yet be important. Unfortunately, there are very few mentions of such species in the literature. Borovikov *et al.*, (2005) allude to data for such species in an earlier publication (Belevantsev *et al.*, 1998) but these are not mentioned at all in the cited report. Calculations involving solutions of 0.58 and 0.11 *m* Sb in 9 *m* HCl (prepared by dissolution of metallic Sb in boiling, concentrated HCl followed by dilution) were illustrated by means of speciation diagrams. At ambient temperatures (20°C), $\text{SbClOH}^+(\text{aq})$ and $\text{SbCl}_2\text{OH}^0(\text{aq})$ contributed approximately 10 and 1%, respectively of total dissolved Sb, but the conditions of the study are far remote from anything that could be encountered in oxidizing Sb deposits. Pokrovski *et al.* (2006) derived stability constants for $\text{Sb}(\text{OH})_3\text{Cl}^-$ and $\text{Sb}(\text{OH})_2\text{Cl}^0$ at 300, 350 and 400°C and SbOHCl_2^0 at 300°C, all at a pressure of 600 bar (stated terms vary above and below the critical point for H₂O). For equations (1.10) and (1.11), $\lg K_{600\text{bar}} = -519.4/T(\text{K}) + 0.8 \pm 0.2$ and $-5000.5/T(\text{K}) + 1.1 \pm 0.5$, respectively, for the given temperature range; $\lg K = -15.1 \pm 1.0$ for equation (1.10) at 300°C.



Extrapolation to 25°C is highly dubious, but gives lg K values of -0.9 and -15.7 for (1.11) and (1.12), respectively. Modelling of species distributions using these values indicates no special significance for them over that pertaining to the SbCl_x^{3-x} species considered above. It is thus considered that such complexes are not relevant to the supergene environment except under exceptional circumstances. These exceptions may pertain to the conditions of formation of the very rare Sb(III) species onoratoite, $\text{Sb}_8\text{O}_{11}\text{Cl}_2$, and nadorite, PbSbO_2Cl . In the latter case lattice energy effects may be more important in the stabilization of the mineral.

Few values are available for chloride complexation to Sb(V), obtained using 5 to 9 *m* HCl to prevent hydrolysis. It is considered that such complexes are not relevant to the supergene environment and that hydrolysed Sb(V) species dominate aqueous speciation for all relevant conditions. However, chloride complexes are no doubt important in Sb transport under hydrothermal conditions at low pH and with high chloride activities.

Antimony in Soils

Thanabalasingam and Pickering (1990) found that the hydrous oxides of Mn, Al and Fe avidly adsorbed Sb from μM solutions of Sb(OH)_3 . Adsorption capacities decreased through the series $\text{MnOOH} > \text{Al(OH)}_3 > \text{FeOOH}$ at acidic pH values and then tapered off. Using saturated solutions of Sb(OH)_3 in potassium antimony tartrate (KSbT) MnOOH had an uptake capacity of $\sim 160 \text{ mmol kg}^{-1}$ at $\text{pH} < 7$. When 0.4 M CH_3COONa was added to the aqueous phase to minimise retention of weakly bound Sb, there was little change in retention on MnOOH, but Al(OH)_3 and FeOOH showed reduced uptake by a factor of about two thirds.

Pilarski *et al.*, (1995) reported the first quantitative data concerning Sb(III) binding to natural organic matter such as humic acid. Humic acid was found to take up Sb(III) as Sb(OH)_3 with a saturation capacity of $23 \mu\text{mol g}^{-1}$ at pH 3.1; Sb(OH)_3 binding was reduced by about 15% at pH 5.4. Buschmann *et al.* (2005) showed that oxidation to Sb(V)

in the presence of humic acid is a feature of the system, which is greatly accelerated by the presence of light and also increases linearly with the concentration of dissolved organic carbon.

Numerous workers (Johnson *et al.*, 2005; Mitsunobu *et al.*, 2006; Steely *et al.*, 2007; Filella *et al.*, 2002a,b, 2003) have shown that Sb(V) is the dominant oxidation state in aqueous solutions in oxic environments and in soils. The adsorption of Sb(V) onto humic acids has been directly tested by Pilarski *et al.* (1995) and Tighe *et al.* (2005), but gave conflicting results. The former found no adsorption on humic acid in acidic solution (actual pH not given) of Sb(OH)_6^- at $<10 \mu\text{mol L}^{-1}$ (2.2 ppm) and only limited sorption thereafter with a maximum of $8 \mu\text{mol g}^{-1}$ (1.8 ppm). This was attributed to the stability of the Sb(OH)_6^- ion, but Filella *et al.* (2002b) reasoned that Sb(OH)_6^- is less likely to interact with humic acid due to its predominately negative charge near neutral pH. Tighe *et al.* (2005) found that humic acid adsorbed up to 60% of available Sb(V) in their experiments at acidic pH values; when the pH was increased this fell to zero. This same study also shed light on the sorption of Sb(V) by Fe(OH)_3 in two different floodplain soils. “ Fe(OH)_3 ” retained $>95\%$ of Sb(V) in all *in vitro* experiments, regardless of pH, and both soils retained $>75\%$ in all trials and 80-100% for pH values <6.5 .

Johnson *et al.* (2005), Leuz *et al.* (2006) and Steely *et al.* (2007) state that the adsorption of Sb(III) and Sb(V) onto iron hydroxides has the ability to arrest Sb within the top layer of the soil if the Sb is penetrating vertically. This was shown to be the case concerning soils contaminated by antimony-bearing lead arsenate pesticides in apple orchards and by bullets in shooting ranges (Sb is used as a hardening agent in lead projectiles). Leuz *et al.* (2006) found that in 0.01 M and 0.1 M HClO_4 solutions the maximum sorption density for Sb(V) on goethite was $136 \pm 8 \mu\text{mol g}^{-1}$ at pH 3. Adsorption was greater than 96 and 80% for Sb(V) at pH 3-6 and Sb(III) at pH 1-12, respectively (reaction conditions $[\text{Sb(V)}]_0 = 4.15 \mu\text{M}$, $[\text{Sb(III)}]_0 = 2.2 \mu\text{M}$, 0.5 g L^{-1} goethite, 25°C). Sb(V) sorption on goethite decreased above pH 6 and for Sb(III) was less at low pH due to the formation of Sb(OH)_2^+ and at high pH due to oxidation to Sb(V). Mitsunobu *et al.* (2006) claimed that under reducing conditions the concentration of antimony decreases in both soil and laboratory experiments and Sb(V) was present at $E = 360$ to -140 mV at pH 8.

The effects of oxidation were tested over time at pH 3, 7.3 and 9.9 by Leuz *et al.* (2006). The concentration of adsorbed Sb(III) remained constant for 35 days at pH 3 and 7.3 with no significant oxidation to Sb(V). At pH 9.9, adsorption decreased by 30% within 7 days, and after 2 further days no significant amount of Sb(III) remained. This indicates that Sb(III) had been oxidised and Sb(V) released into solution. At pH 3, 5.9 and 9.7, much more rapid oxidation (10 days) of Sb(III) occurred when the goethite was dissolved in oxalic-ascorbic acid solutions, though significant Sb was still bound to goethite at high concentrations. Except for very localised environments, pH values >9 are not common, especially in the vicinity of oxidising sulfide deposits. Over the range of the vast majority of natural soil pH conditions the experiments demonstrate that Sb should be relatively immobile in Fe oxide- and humic acid-rich soils and Sb(V) species will dominate. It should also be noted that the formation of initially amorphous precipitates that recrystallise to more thermodynamically stable pyrochlore-type or other minerals over time may create a false impression of the importance of sorption effects especially near oxidising ores where Sb concentration may be very high.

Taking all of the above into account, the striking gap in our knowledge of the behaviour of Sb in the supergene environment concerns the dearth of data for Sb(V) minerals that are known to occur in such settings and the role that they may play in buffering Sb solubility and transport in soil or surface waters. The main aim of this thesis was to, in part, rectify this deficiency by determining the solubilities of the Sb(V) minerals brandholzite, bottinoite, roméite and bindheimite. This has been achieved, and supplemented by synthetic studies related to Fe(II) and Fe(III) minerals that also contain Sb(V).

Conclusions based on these studies (*viz*, Sb is quite immobile in the supergene setting) have been validated in an orientation soil geochemical survey over known Sb mineralisation. Metastable sorption of Sb on amorphous Fe(III) oxyhydroxides has been noted in the field and the studies were further elaborated by identification of secondary Sb mineral assemblages in a number of deposits.

CHAPTER 2 EXPERIMENTAL

Measurements

X-ray powder diffraction studies were carried out using a Philips PW1825/20 diffractometer (Ni-filtered Cu $K\alpha_1$ radiation, $\lambda = 1.5406 \text{ \AA}$, 40 kV, 30 mA). Traces were produced between $5\text{-}70^\circ 2\theta$, with a step size of 0.02° and a speed of $1.2^\circ \text{ min}^{-1}$. Diffraction Technology Data processing software (Traces Version 6) and JCPDS-ICDD data base files were used to identify crystalline phases.

A JEOL JXA-840 scanning electron microscope fitted with an energy dispersive detector was used for solid state analyses (20 kV, 2 nA) and to capture back-scattered and secondary electron images. Moran Scientific acquisition, control and processing software was employed. Samples were carbon coated in a vacuum chamber prior to analysis.

TGA measurements were made using a Bruker–Vertex 70 instrument (Al_2O_3 crucible, $25\text{-}900^\circ\text{C}$, $10^\circ \text{ min}^{-1}$, argon). All samples were dried in the oven at 140°C for 4 days prior to analysis to liberate free water. IR spectra (KBr pellets) were recorded on a Perkin Elmer Spectrum One FT-IR spectrophotometer.

Solubilities of brandholzite and bottinoite were determined by AAS (Mg, Ni) using a Perkin Elmer AAnalyst100 spectrophotometer (air-acetylene, 2000 ppm added KCl to control ionization, matched standards). ICP-MS (Sb and Pb) and ICP-OES (Ca) analyses were determined by a NATA-compliant commercial laboratory (LabMark PL, Asquith, Australia). Soil analyses were carried out by a NATA-compliant commercial laboratory, Australian Laboratory Services PL, Brisbane, Australia, using ICP-MS and -OES methods.

Measurements of pH were made using a Radiometer PHM220 apparatus fitted with a combination electrode.

Syntheses

Bottinoite and Brandholzite

An aqueous 0.100 M solution of $\text{Sb}(\text{OH})_6^-$ solution was made by refluxing $\text{KSb}(\text{OH})_6(\text{s})$ in water for 2 hours. A small amount of undissolved material was separated by decantation. Aliquots of the above solution were mixed with 0.100 M aqueous solutions of $\text{MgCl}_2 \cdot 6\text{H}_2\text{O}(\text{s})$ or $\text{Ni}(\text{NO}_3)_2 \cdot 6\text{H}_2\text{O}(\text{s})$ at a mol ratio of Sb:Mg,Ni equal to 2:1. In both cases X-ray amorphous precipitates formed immediately and the mixtures were left to stand at room temperature. In the case of the Mg preparation, squat, hexagonal prisms of brandholzite, $[\text{Mg}(\text{H}_2\text{O})_6][\text{Sb}(\text{OH})_6]_2(\text{s})$, up to 1 mm in size were obtained overnight. The product was left to age further for 1 month, washed by decantation, collected at the pump, washed with water and acetone, sucked dry, then finally dried in an oven at 40°C. In the Ni case a few crystals could be seen in the precipitate after 24 hours. The precipitate was left to age during 1 month, when it had converted to pale green, hexagonal plates of bottinoite, $[\text{Ni}(\text{H}_2\text{O})_6][\text{Sb}(\text{OH})_6]_2(\text{s})$. The product was isolated as above. Yields of brandholzite and bottinoite were >90%. XRD measurements showed that the minerals were not contaminated with any other detectable phases. Traces were indexed and unit cell data refined using LAPOD (Langford, 1973). For brandholzite and bottinoite, both cells were hexagonal with $a = 16.124(1)$, $c = 9.874(1)$, and $a = 16.070(2)$, $c = 9.800(1)$ Å, respectively. These values compare excellently with those reported earlier (Bonazzi *et al.*, 1992; Friedrich *et al.*, 2000).

Roméite and Bindheimite

Aqueous 0.100 M solutions of $\text{PbNO}_3(\text{s})$ or $\text{Ca}(\text{NO}_3)_2 \cdot 4\text{H}_2\text{O}(\text{s})$ were mixed with the above solution of $\text{Sb}(\text{OH})_6^-$ at Sb:Pb,Ca mol ratios of 1:1 or 1:2. In all cases, white, flocculent precipitates were obtained and remained X-ray amorphous at room temperature for more than 2 months. To accelerate ageing the mixtures were refluxed. After 1 hour dense precipitates were obtained (white for the Ca salts and pale yellow to tan in colour for the Pb salts). The mixtures were refluxed for a further 11 hours and the resulting precipitates separated by centrifuging and decanting. Products were washed several times with water, then acetone, and dried in the oven at 40°C. Yields were essentially quantitative. Powder XRD showed that all species had the pyrochlore structure (stibiconite group) and SEM analyses indicated that the solids had Sb:M (M = Ca, Pb) ratios corresponding to those used

in the synthesis. Thus the compositions $MSb_2O_5(OH)_2$ and $M_2Sb_2O_7$ ($M = Ca, Pb$) were obtained. XRD traces were indexed by analogy to other stibiconite group minerals and unit cell data refined using LAPOD (Langford, 1973). $CaSb_2O_5(OH)_2$, $Ca_2Sb_2O_7$, $PbSb_2O_5(OH)_2$ and $Pb_2Sb_2O_7$ gave $a = 10.277(2)$, $10.289(2)$, $10.417(2)$ and $10.452(6)$ Å, respectively, in excellent agreement with literature values (Anthony *et al.*, 1990-2003).

Tripuhyite and an Fe(II)-Dominant Member of the Stibiconite Group

A 0.10 M aqueous solution of $Fe(NH_4)_2(SO_4)_2 \cdot 6H_2O$ was mixed with the $KSb(OH)_6$ solution mentioned above in a 1:2 Fe:Sb mol ratio. A brown X-ray amorphous precipitate formed immediately and the mixture was refluxed overnight. XRD measurements of the isolated solid showed it to be poorly crystalline tripuhyite, $FeSbO_4$.

In order to form an Fe(II) member of the stibiconite group, it was reasoned that the lattice could be stabilised by the presence of large cations such as Pb^{2+} or Ca^{2+} . Iron powder was dissolved in glacial acetic acid and AAS used to determine the Fe concentration. The solution was mixed with aqueous 0.10 M $PbNO_3$ at a series of Pb:Fe mol ratios (1:1, 1:2, 1:2.5, 1:5, 1:10, and 1:20) and then with the $KSb(OH)_6$ solution in a 1:2 Fe+Pb:Sb mol ratio. Solids isolated from the 1:1, 1:2, 1:2.5 Pb:Fe mol ratios produced the pyrochlore XRD pattern with $a = 10.385(3)$, $10.390(3)$ and $10.388(2)$ Å, respectively. The other runs gave poorly crystalline tripuhyite.

Solubility Studies

Bottinoite and Brandholzite

Bottinoite or brandholzite (*ca* 0.2 g) was added to 100 cm³ of water in sealed conical Quickfit flasks and left to equilibrate at $25 \pm 0.2^\circ C$ in a thermostatted water bath. Separate solutions were monitored periodically for dissolved Ni or Mg until no change in concentration was detected (*ca* 1 week). After 30 days, the pH of the solutions was measured and the solutions filtered (0.2 µm) and analysed by AAS for Ni or Mg. Separate experiments (XRD) showed that bottinoite and brandholzite dissolve congruently in water. A separate batch of solubility experiments was run using 0.100 M KNO_3 as background electrolyte.

Roméite and Bindheimite

Accurate amounts of bindheimite or roméite ($M_2Sb_2O_7$, 0.5 g) were placed in sealed conical Quickfit flasks together with 100.000 g of 0.0100 M aqueous HNO_3 and left to equilibrate at $25\pm 0.2^\circ C$ in a thermostatted water bath. Separate solutions were monitored periodically for pH until no change was detected (*ca* 1 day). After 14 days the final pH values were recorded and the solutions filtered as above. Dissolved Ca, Pb and Sb concentrations were then determined by ICP methods.

Mineral and Water Samples

Rock and mineral samples were collected purely on a visual basis; no systematic sampling approach was followed. Samples were collected from both current and historic mine sites in the Hillgrove ore field and at the Razorback mine. Specimens from a number of private collections and museum collections were also studied. Any minerals of interest were hand-picked and identified by XRD. In the 1720 level of the syndicate lode so-called antimony ochres were found as stalactites on the back of the drive near massive stibnite mineralisation. These were identified by XRD and SEM methods.

Underground water samples (1 L) were collected on 2 drives on the Syndicate lode at Hillgrove. Sample 4/1 was collected on the 1830 level from drips of the ceiling where a vein up to 30 cm of massive stibnite mineralisation was visible. Sample 6/1 was taken from the 1740 level from a sub-horizontal diamond drill hole (BLK011). This drill hole was in the northern wall and cut the stibnite-rich Black lode approximately 10 m away. The pH of each sample was recorded on site, filtered (0.2 μm) and the filtrate sent to LabMark PL for analysis.

Soil samples for the geochemical orientation survey over the Bayley Park prospect were taken from the B horizon, sieved (minus 1.25 mm) and assayed for a suite of elements by ICP-MS by the NATA-compliant commercial laboratory, Australian Laboratory Services PL, Brisbane, Australia. These samples on lines perpendicular to the known sub-vertical mineralised shear were located spatially using GPS with a resolution of 3 m.

CHAPTER 3 FIELD SITES AND SETTINGS

Hillgrove, New England, New South Wales

The New England region has a rich mining history. There are 940 recorded mineral deposits within the Dorrigo-Coffs Harbour 1:250,000 sheet area (Gilligan *et al.*, 1992). Metallogenesis is dominated by antimony and gold, but deposits of silver, arsenic, base metals, mercury, magnesium and graphite are also found in the area.

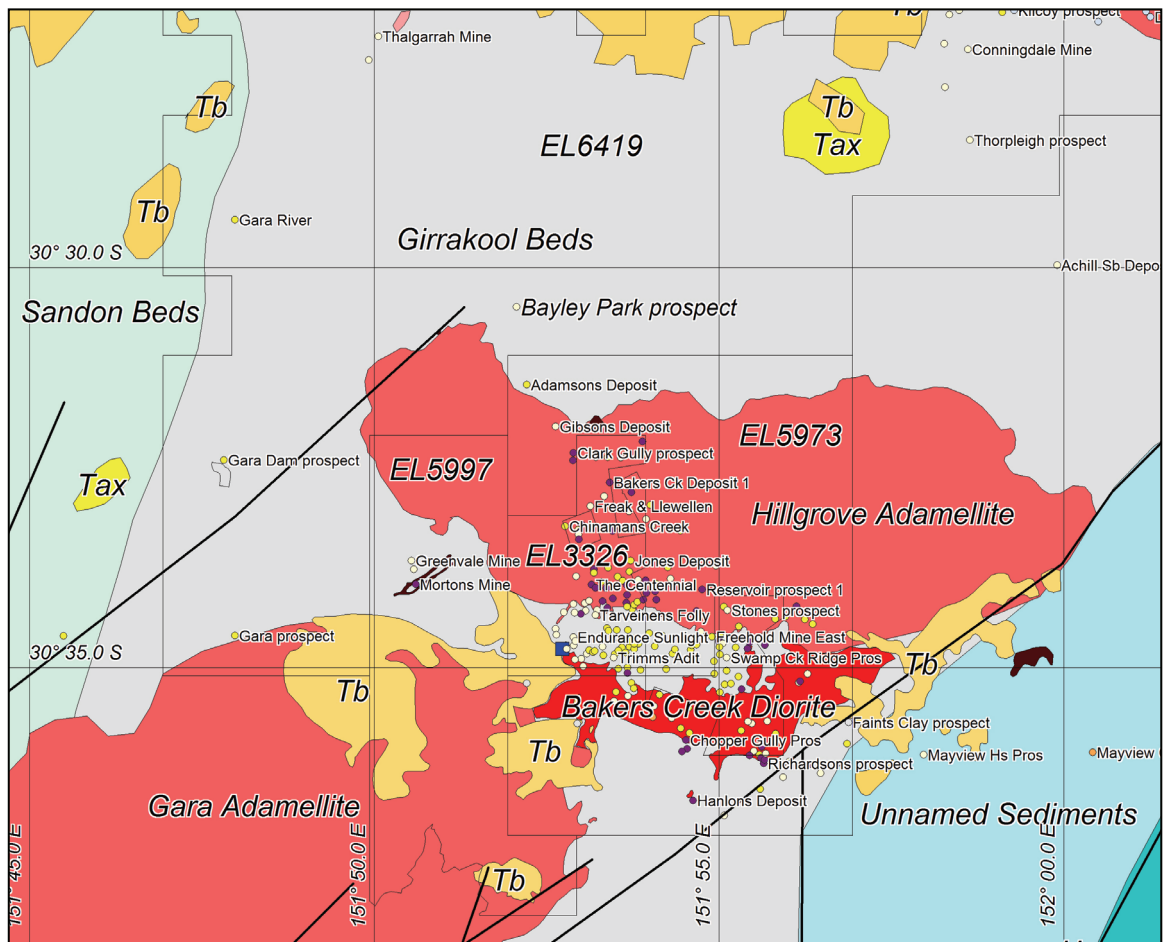


Figure 3.1. Geology of the Hillgrove area, New South Wales.
Source: Straits Hillgrove Gold.

Occurrences of semi-precious stones commonly attract fossickers and important industrial and construction materials have also been exploited. A geological map of the area is shown in Figure 3.1. Also shown are the locations of several deposits that have been examined during the course of this study.

The historic mining town of Hillgrove is located some 24 km East of Armidale at the northern head of the Bakers Creek gorge and sits at about 1,000 m ASL. The Reverend W.B. Clarke first noted antimony at Hillgrove in 1853, although mining did not commence until 1877 when the Evershed brothers and one Mr Thomas discovered the Syndicate reef (Gilligan *et al.*, 1992). A major boom began when gold was discovered at the Garibaldi and Eleanora mines in 1881. Four years later the Bakers Creek, Sunlight, and Cosmopolitan North and South gold mines were developed. By the early 1890s, Hillgrove and Metz were thriving mining communities, with a population larger than that of Armidale. There are some 194 deposits recorded in the immediate Hillgrove area and mining there was continuous for 40 years. In 1971, larger scale mining recommenced when New England Antimony Mines NL (NEAM) developed Smith's mine. NEAM also worked the Freehold, Brereton Falls, Freehold East and Eleanora mines (Gilligan *et al.* 1992) until 2002. Total recorded production from the Hillgrove field to June 1991 is 21,530 kg of gold, 46,058 tonnes of antimony and 2,100 tonnes of scheelite (Ashley *et al.*, 1993). In March 2004, Straits Resources Ltd (SRL) purchased the Hillgrove Mine from Antimony Resources Australia Ltd (ARA) and in 2006 announced they would commence construction of a plant capable of achieving initial production rates of 10,000 tonnes of antimony and 20,000 ounces of gold per annum, plus 30 tonnes of scheelite concentrates (SRL ASX Preliminary final report, 2008). Commissioning of the mine commenced in late 2007 (Simpson, 2007).

The Hillgrove mineral field lies in the western half of the Nambucca Block (Comsti and Taylor, 1984) in the southern portion of the Late Palaeozoic to Mesozoic New England Orogen of eastern Australia. Much of the central region of the southern New England Orogen is composed of Mid to Late Palaeozoic sedimentary complexes, which had been amalgamated by the Early Permian. Episodic intrusions of granitic batholiths followed during the Late Carboniferous to Late Triassic, accompanied by some felsic volcanism. The mineral field sits in an east-west trending metasediment wedge, between two S-type granitoids of the Hillgrove Plutonic Suite of Late Carboniferous (~300 Ma) to Early Permian age.



Figure 3.2. Entrance to the main decline to the Syndicate lode on the Metz side of the Bakers Creek gorge (June, 2008). Photo: P.A. Williams

Both the Hillgrove Adamellite and the Bakers Creek Diorite are cut off and displaced on their south-east boundary by the north-east trending Chandler Fault. The intrusions are often stressed and foliated with similar structural trends as the Gurrakool Beds (Comsti and Taylor, 1984). The Hillgrove Adamellite is characterised by bluish quartz and large K-feldspar phenocrysts and ranges from a coarse grained, foliated biotite adamellite (quartz monzonite) to a granodiorite. Bakers Creek Diorite varies in composition from diorite to tonalite and graphite is common in shear planes, occurring in patches up to 5 cm across.

The Gurrakool Beds are part of a Palaeozoic accretionary complex (Ashley and Craw, 2004) and are the oldest rocks in the Hillgrove area. They are composed of dark slates, siliceous cherty argillites, siltstone and greywackes, which have been regionally deformed and metamorphosed to lower greenschist facies, resulting in chlorite and white mica as matrix recrystallisation products. Close to the contacts of the Hillgrove and Gara Adamellites abundant metamorphic biotite occurs and in the more pelitic sediments spotted hornfels containing cordierite patches up to 2 mm across have been observed (Simpson, 2007).

Mineralisation occurs as the primary antimony sulfide stibnite (Sb_2S_3), gold and scheelite (CaWO_4) in lodes as veins, stockworks and shears dipping sub-vertically to the south. Lode thickness varies up to 10 m, with strike length highly variable in a mineralised zone up to 20 km in extent. Individual shoots up to 100 m long fill pinch and swell structures. All rock types are intruded by aplite and lamprophyre dykes, pre-, syn-, and post-mineralisation and these are believed to be Permian in age (Simpson, 2007). Further away from the intrusive rocks, many smaller Sb prospects are known. These are, as far as is known, fault-hosted.

The Bayley Park prospect (Figure 3.3) is located 8 km NW of Hillgrove (Figure 3.1). Stibnite mineralisation occurs in a sub-vertical quartz breccia-filled shear in metasediments approximately 1 km north of their contact with the Hillgrove Adamellite. In 1971 Anglo Range NL excavated 17 shallow costeans (max depth 0.9 m) across the lode and sank a vertical shaft to 14 m. No mining was undertaken and the costeans were back-filled (Hall, 1972).



Figure 3.3 The Bayley Park prospect site (June, 2008). An old prospecting pit is located 20 m to the left of the car bonnet. Photo: G.A. Diemar

Many other deposits and mines of the Hillgrove area were visited during this study, including Syndicate reef, Black Lode, Middle reef, Sunlight lode, Oscars Reef, Bakers Creek mine, Eleanora mine, the Lower Cooney mine, Clarks Gully prospect, Chinamans Gully prospect, Damifino mine, Becks Spur prospect and Becks Gold prospect, Fishers antimony mine, Fishers scheelite mine, Keys mine, Conningdale mine, Rockvale arsenic mine, Thalgarrah mine, and many small unnamed prospects. Many of these are located in extremely rugged terrain (Figure 3.4). Almost 7000 m of diamond drill core from the Eleanora, Brackins Spur and Syndicate lodes was geologically logged in order to gain a firm understanding of the geology.



Figure 3.4. Bakers Creek gorge looking east from the entrance of Fishers antimony mine. Photo: P.A. Williams

Razorback Mine, Lachlan Fold Belt, New South Wales

The Razorback mine is located about 70 km northwest of Lithgow, beside the Razorback Road that joins the villages of Sofala and Cherry Tree Hill, New South Wales. The workings are 8 km from Cherry Tree Hill. The first mining lease over the deposit was granted in 1881, but there is a report of several shafts being sunk by one O'Brien and party in 1876 (Staude, 1970). Workings stretch intermittently for approximately 500 m in a north to northwest direction. It is reported that "472 tonnes of ore containing 45-90 tonnes of antimony and several hundred ounces of gold" were won between 1881 and 1904 (Staude, 1970; Clarke and Raphael, 1982). Mine development consisted of a main shaft to a depth

of 101 m and five levels at 15, 27, 44, 77, and 101 m (Staude, 1970; Carne, 1903). There are 3 known and 3 other possible small shafts all within 200 m of the main shaft; all have been back-filled. A total of 27 samples were taken the deposit and produced mean values of 11.8% Sb and 26.1 ppm Au (Clarke and Raphael, 1982). These values probably overestimate the grade since they include high values from bulk samples that were sorted prior to despatch and one highly anomalous Au value of 126.1 ppm. Limited exploration in 1970 and 1982 estimated a resource of 7,400 tonnes of lode material at a rough net grade of 8% Sb and 17 ppm Au. No drilling has been completed over the deposit (Staude, 1970; Clarke and Raphael, 1982).

The Razorback lode is a quartz-calcite-stibnite vein in the Sofala Volcanics (Ordovician age) striking 350° and dipping to the west at about 60°. In the vicinity of the mine, black shales have a similar north-south strike. One kilometre to the east, the Sofala Volcanics are faulted on a northerly strike against sediments of the Devonian Lambie Group. The lode channel is approximately 500 m long and may be made up of two or three separate mineralised veins. Mineralisation ranges in width from 5 cm to 1 m, with an average of 30 cm.

CHAPTER 4 RESULTS

A Possible New Stibiconite Group Mineral from Broken Hill, New South Wales

During the course of other synthetic studies, attention was drawn to an extremely fine-grained, yellow mineral surrounding chlorargyrite, AgCl, from the Australian Broken Hill Consols mine, Broken Hill, New South Wales. The material in hand specimen was Sb-rich and was the oxidised equivalent of primary dyscrasite, Ag₃Sb (Smith, 1922; Plimer, 1982). XRD analysis showed this mineral to have the pyrochlore structure with a cell comparable to, but slightly smaller than, that of bindheimite. Microprobe analysis (Appendix 1; Ian Graham, personal communication) accounted for 84% of the weight as metal oxides with the remainder thought to be due to H₂O. The approximate formula of the material, calculated on the basis of the general pyrochlore formulation, was Fe₂Sb₂O₇. Because the polished slab containing this mineral was porous good analyses were difficult to obtain; also only very small amounts were available for study. This made it impossible to measure its physical and optical properties and carry out any further required analyses to account for the low analytical total. A confidential submission in 2004 to The Commission on New Minerals, Nomenclature and Classification (CNMNC) of the International Mineralogical Association (IMA) was rejected due to these reasons.

The synthetic routes developed for bindheimite and roméite were thought, by the author, to possibly provide a method for making enough material for accurate analysis and determination of the remaining physical properties. Attempts to synthesise the material having the ideal formula (Fe₂Sb₂O₇) with a pyrochlore structure gave poorly crystalline tripuhyite. Nevertheless, the Fe-rich Sb pyrochlore was able to be obtained if sufficient Pb²⁺ was present and it became evident that a large cation such as Pb²⁺ is necessary to stabilise the cubic pyrochlore lattice. Oven-dried (140°C, 4 days) samples examined by FTIR showed the presence of OH⁻, which explains in part the missing mass in the analysis of the natural material. It also indicated that the material has a defect structure if a total of 2 divalent cations per formula unit are present.

At this stage, only a simplified formula can be proposed and complete resolution of the problem awaits further analysis. This potential new mineral would be (hypothetically) the

Fe(II) end-member of a series to bindheimite, based on the 50% rule. The proposed formula is $(\text{Fe}^{\text{II}}_{2-x}\text{Pb}_x, \square)_2\text{Sb}_2\text{O}_6(\text{O}, \text{OH})$ with x greater than about 0.2. A second submission to the CNMNC is being written to have the compound validated as a new mineral species.

Other Mineral Syntheses

Both brandholzite and bottinoite have been synthesised previously in small yield (Jander and Brüll, 1926; Beintema, 1936; Williams, 1985; Bonazzi *et al.*, 1992; Friedrich *et al.*, 2000, 2003; Palenik *et al.*, 2005). It has been found that the simple expedient of letting the initially-formed X-ray amorphous precipitates age at ambient temperatures in contact with mother liquor markedly improves yield and large crystals were obtained. SEM images of these are shown in Figures 4.1 and 4.2. Hexagonal habits can be clearly seen.

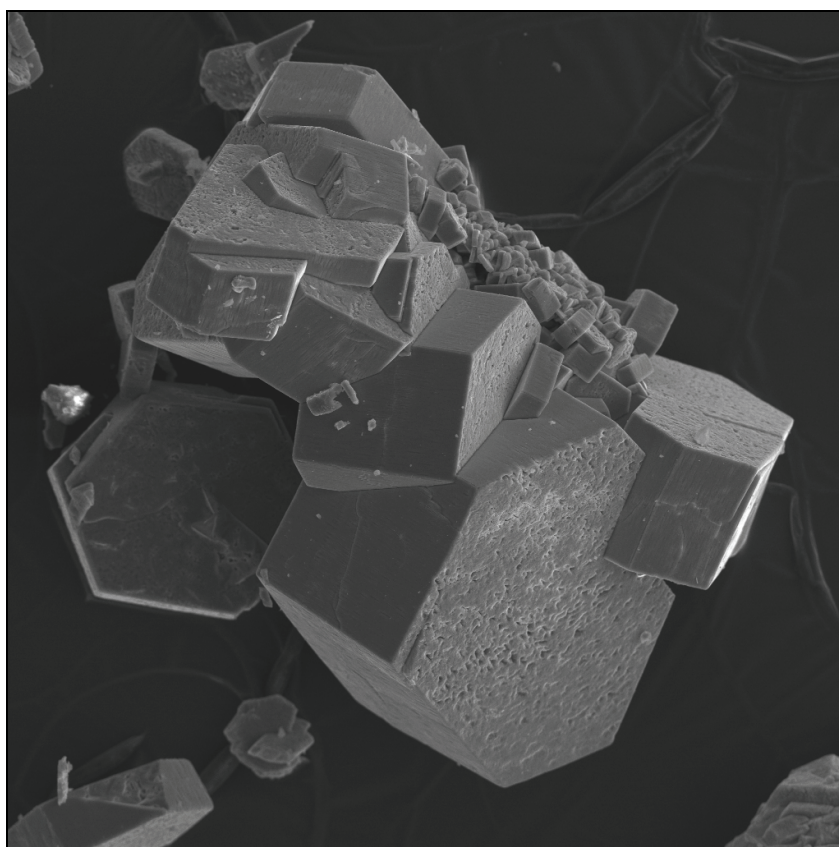
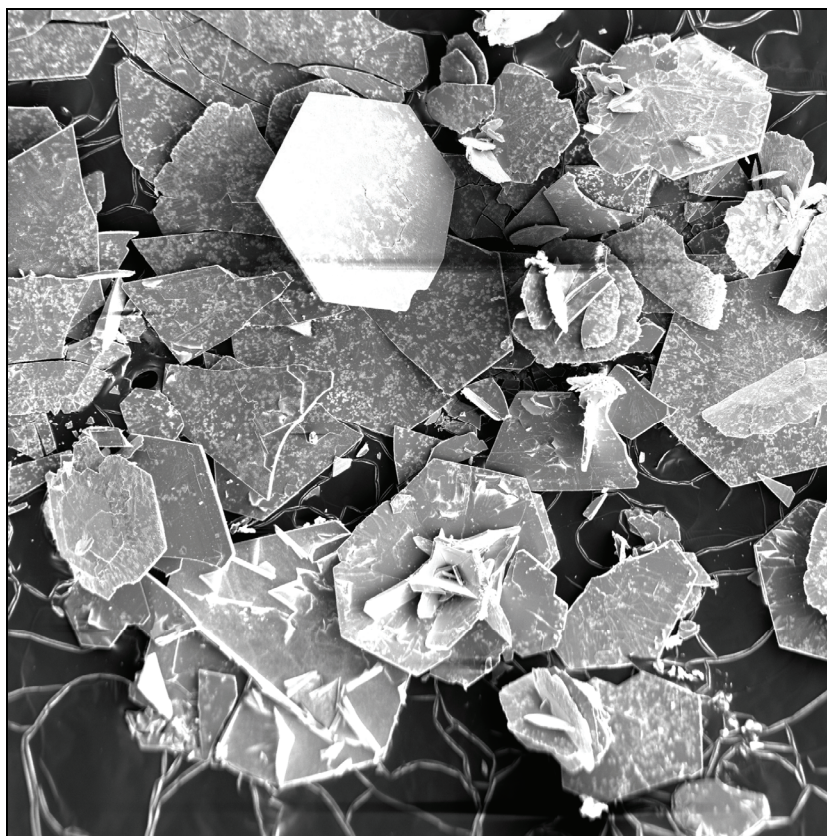


Figure 4.1. SE image of a cluster of synthetic brandholzite crystals. Field of view is 1.7 mm.



**Figure 4.2. SE image of synthetic bottinoite crystals.
Field of view is 5 mm.**

As noted above, solid state synthetic routes for end-member roméite and bindheimite are available (Brissé *et al.*, 1972) and they may be also prepared by cation exchange of the cubic antimonite acid $\text{Sb}_2\text{O}_5 \cdot 4\text{H}_2\text{O}$ (Baetsle and Huys, 1968; Abe, 1979). The syntheses developed here are the first to directly precipitate from aqueous solution and this is significant in that the route mimics what must occur in Nature. It is also noteworthy that the ionic radii of the cations in the salts of $\text{Sb}(\text{OH})_6^-$ control the structures obtained. Na^+ ($r = 102$ pm (Alyward and Findlay, 2002) for 6-fold coordination) gives mopungite, but charge considerations are important and stoichiometries are necessarily different for divalent cations. Mg^{2+} and Ni^{2+} ($r = 72$ and 69 pm (Alyward and Findlay, 2002), respectively, for 6-fold coordination) give the isomorphous layered hexagonal phases brandholzite and bottinoite. In order to stabilise the pyrochlore lattice it is evident that rather larger cations are required ($r = 112$ and *ca* 119 pm (Alyward and Findlay, 2002), respectively, for Ca^{2+} and Pb^{2+} in 8-fold coordination).

Fe^{2+} does not give rise to a brandholzite/bottinoite-like phase under ambient conditions. Rather, it is oxidised to Fe^{3+} and tripuhyite results. Again this is pleasing in that the synthesis from aqueous solution of the mineral is the first of its type and mirrors how the

mineral forms in the supergene environment. Tripuhyite is also known as a high temperature pegmatite phase (Anthony *et al.*, 1990-2003).

Solubility Studies

Results concerning the solubilities of bottinoite and brandholzite in water at 298.15 K are given in Tables 4.1 and 4.2, respectively. Both were found to dissolve congruently.

Table 4.1. Final Ni²⁺ concentrations for filtrates obtained from the dissolution of bottinoite in water at 298.15 K, and equilibrium pH values.

Solution	[Ni]/ppm	[Ni]/mol dm⁻³	pH
1	20.37	3.47 x 10 ⁻⁴	5.72
2	20.89	3.56 x 10 ⁻⁴	5.83
3	19.59	3.34 x 10 ⁻⁴	5.86
4	19.58	3.34 x 10 ⁻⁴	5.80
Average	20.11	3.42 x 10 ⁻⁴	5.80
SD	0.64	1.09 x 10 ⁻⁵	0.06

Table 4.2. Final Mg²⁺ concentrations for filtrates obtained from the dissolution of brandholzite in water at 298.15 K, and equilibrium pH values.

Solution	[Mg]/ppm	[Mg]/mol dm⁻³	pH
1	46.50	1.91 x 10 ⁻³	6.12
2	48.40	1.99 x 10 ⁻³	6.05
3	48.20	1.98 x 10 ⁻³	6.07
4	46.50	1.91 x 10 ⁻³	6.22
Average	47.40	1.95 x 10 ⁻³	6.12
SD	1.04	4.29 x 10 ⁻⁵	0.08

Individual ion activity coefficients have been calculated using the Davis extension of the Debye-Hückel equation $\lg \gamma = -Az^2(\sqrt{I}/(1+\sqrt{I}) - 0.3I)$. ΔfG^0 data for cations and water at 298.15 K and are taken from Robie and Hemingway (1995), except for Sb(OH)₆⁻(aq). A value for the latter was derived earlier; it is assigned an arbitrary but reasonable error of ± 1.0 kJ mol⁻¹ in further calculations. K_{SP} terms refer to expression (4.1).



From the solubility experiments, the solubility of brandholzite in water is equal to $1.95(4) \times 10^{-3}$ mol dm⁻³ at 25°C [$n = 4$; pH = 6.12(8); $I = 5.85(4) \times 10^{-3}$; $\gamma^{2\pm} = 0.723$; $\gamma^{\pm} = 0.922$], and this yields $K_{SP} = 1.82 \pm 0.15 \times 10^{-8}$ and $\Delta fG^0(\text{brandholzite}, s, 298.15K) = -4358.4 \pm 3.4$ kJ

mol⁻¹. Similarly, the solubility of bottinoite in water is equal to $3.42(11) \times 10^{-4}$ mol dm⁻³ at 25°C [n = 4; pH = 5.80(6); $I = 1.03(11) \times 10^{-3}$; $\gamma^{2+} = 0.866$; $\gamma^{\pm} = 0.965$], and this yields $K_{SP} = 1.29 \pm 0.13 \times 10^{-10}$ and $\Delta fG^{\circ}(\text{bottinoite}, s, 298.15\text{K}) = -3961.1 \pm 3.7$ kJ mol⁻¹. It should be noted that at the pH values given above, the concentrations of hydrolysed Ni²⁺(aq) species and Sb(OH)₅⁰(aq) can be neglected in the calculations (Smith and Martell, 1976; Accornero *et al.*, 2008); check calculations using COMICS (Perrin and Sayce, 1967) verified this fact.

The solubilities of bottinoite and brandholzite in aqueous 0.1 M KNO₃ at 298.15 K are given in Tables 4.3 and 4.4, respectively.

Table 4.3. Final Ni²⁺ concentrations for filtrates obtained from the dissolution of bottinoite in 0.10 M KNO₃ at 298.15 K, and equilibrium pH values.

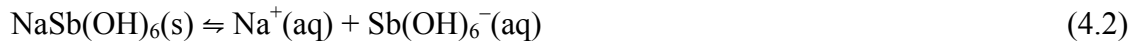
Solution	[Ni]/ppm	[Ni]/mol dm ⁻³	pH
1	31.56	5.38×10^{-4}	5.58
2	32.70	5.57×10^{-4}	5.64
3	32.30	5.50×10^{-4}	6.19
4	32.46	5.53×10^{-4}	5.47
Average	32.26	5.49×10^{-4}	5.72
SD	0.49	8.37×10^{-6}	0.32

Table 4.4. Final Mg²⁺ concentrations for filtrates obtained from the dissolution of brandholzite in 0.10 M KNO₃ at 298.15 K, and equilibrium pH values.

Solution	[Mg]/ppm	[Mg]/mol dm ⁻³	pH
1	55.70	2.29×10^{-3}	5.78
2	57.50	2.37×10^{-3}	5.86
3	64.20	2.64×10^{-3}	5.83
4	59.80	2.46×10^{-3}	5.81
Average	59.30	2.44×10^{-3}	5.82
SD	3.67	1.51×10^{-4}	0.03

In aqueous 0.100 M KNO₃, the solubilities of brandholzite and bottinoite at 25°C were found to be $2.44(15) \times 10^{-3}$ [n = 4; pH = 5.82(3)] and $5.49(8) \times 10^{-4}$ [n = 4; pH = 5.72(32)], respectively. Use of the same method as above to calculate activity coefficients at $I = 0.1$ gives K_{SP} values of 1.33×10^{-8} and 1.51×10^{-10} , for brandholzite and bottinoite, respectively. These are comparable to the values found in water alone, but it is evident that the empirical method used for calculation of activity coefficients cannot be relied upon under these conditions.

Blandamer *et al.* (1974) reported the solubility of mopungite as $3.18 \pm 0.2 \times 10^{-3} \text{ mol dm}^{-3}$ at 25°C. Assuming negligible hydrolysis of the Na^+ ion and concentration of Sb(OH)_5^0 , at this temperature $K_{\text{SP}} = 8.89 \times 10^{-6}$ (4.2) and $\Delta fG^0(\text{mopungite}, \text{s}, 298.15\text{K}) = -1508.5 \pm 1.4 \text{ kJ mol}^{-1}$. At 25°C, the solubilities of the minerals follow the series mopungite > brandholzite > bottinoite, but all three have appreciable solubility.



A somewhat different pattern of solubility emerges for bindheimite and roméite. At 25°C, $\text{Pb}_2\text{Sb}_2\text{O}_7$ equilibrated with 0.0100 M HNO_3 gives a final pH of 2.05 ± 0.05 ($n = 6$), total dissolved Pb equal to $4.12 \pm 0.13 \times 10^{-5} \text{ mol dm}^{-3}$ (*ca* 8.5 ppm) and total dissolved Sb equal to $7.7 \pm 2.1 \times 10^{-8} \text{ mol dm}^{-3}$ (*ca* 9.3 ppb). Similarly, $\text{Ca}_2\text{Sb}_2\text{O}_7$ equilibrated with 0.0100 M HNO_3 gives a final pH of 2.23 ± 0.01 ($n = 6$), total dissolved Ca equal to $2.11 \pm 0.05 \times 10^{-3} \text{ mol dm}^{-3}$ (*ca* 85 ppm) and total dissolved Sb equal to $3.3 \pm 1.0 \times 10^{-7} \text{ mol dm}^{-3}$ (*ca* 40 ppb). Because the salts dissolve incongruently, no free energy values have been derived. Solubility relations are discussed in detail in the following chapter.

Mineral and Water Samples

Water sample 4/1 was collected on the 1830 level of the Syndicate mine, Hillgrove, dripping from partially oxidised massive stibnite mineralisation. The temperature was 13.9°C and the pH was 8.08. Sample 6/1 was taken from the 1740 level from a sub-horizontal diamond drill hole intersecting similar lode material about 10 m distant. The temperature was 16.9°C and the pH was 6.87. Total Sb, As and major cation concentrations in the filtered samples are listed in Table 4.5. It is noteworthy that, even in the immediate vicinity of the oxidising, stibnite-rich mineralisation, dissolved Sb levels are very low. Much higher As concentrations reflect the presence of arsenopyrite, FeAsS , in the lode and the fact that As is much more geochemically mobile than Sb. Major cation concentrations are normal for ground waters associated with acidic rocks (Apello and Postma, 1993).

Table 4.5. Analytical data for the ground water samples.

Sample ID	Sb/ppb	As/ppm	Ca/ppm	Mg/ppm	Na/ppm	K/ppm
4 / 1	3.46	215	183	63.2	23.3	2.6
6 / 1	0.66	13	308	175	50.9	4.1

On the 1720 level, water dripping from the back had too slow a flow rate to make sample collection practicable. The area was characterised by the formation of soft, yellow to orange, Fe-rich stalactites (Figure 4.3). Powder XRD showed the stalactites to be

amorphous but SEM/EDS measurements indicated that they contained significant amounts of Sb. These ochres will ultimately age to form more insoluble secondary antimony minerals.



Figure 4.3: Amorphous, Sb-rich Fe oxyhydroxide ochre stalactites in the back of the 1720 level, Syndicate lode, Hillgrove. Field of view is approximately 1 m across. Photo: P.A. Williams

The stalactites are related to other oxidised material recovered from the small dump associated with the 1971 shaft at the Bayley Park prospect. Some samples of quartz-cemented lode breccia were found that contained vughs filled with a bright orange powder after sulfides. These no doubt came from the upper section of the oxidised profile. Powder XRD measurements revealed that the only crystalline phases present in the orange material were quartz and muscovite mica. SEM/EDS measurements, however, showed that the most volumetrically abundant elements present aside from oxygen were Fe, Sb and As.

Secondary minerals identified by powder XRD from several deposits are listed below, together with their paragenetic relationships. For localities of these mines and prospects, see the Experimental section.

At the Bayley Park prospect quartz-cemented lode breccia containing rock clasts and stibnite was collected from a low rubble pile by an old shaft at the side of the access road and from the small 1971 shaft collar dump. Much but not all of the sulfide mineralization

is replaced by secondary phases, which are invariably associated with lode breccia and not invasive in host metasediments. Yellow- to orange-brown, warty to powdery masses up to 12 mm across on the outer surface of some specimens are mixtures of natrojarosite, $\text{NaFe}_3(\text{SO}_4)_2(\text{OH})_6$, and hydronium jarosite, $\text{H}_3\text{OFe}_3(\text{SO}_4)_2(\text{OH})_6$. The presence of these phases is indicative of an acid oxidising environment. Pale buff to yellow material pseudomorphous after stibnite in lode breccia was shown to be stibiconite-roméite. Mixtures of stibiconite and roméite were also found in vughs in shear breccia (yellow) together with radiating groups of cervantite crystals up to 1 mm in length, pseudomorphous after stibnite. Quartz-stibnite breccia with fine white stibiconite-roméite in contact with stibnite was noted in another specimen. A mixture of sénarmontite, traces of cervantite and stibiconite-roméite was found in yellow coatings immediately adjacent to remnant stibnite. An innermost coating of cervantite on stibnite was found in other samples. Dull, brown outer layers more remote (mm) from stibnite cores consisted of a stibiconite group mineral and minor tripuhyite. Tripuhyite was also identified as resinous, dark brown coatings in vughs associated with stibiconite-roméite, in which sulfide mineralisation had been completely oxidised.

Quartz-cemented lode breccia with rock clasts and stibnite were collected from a dump at the mouth of a collapsed adit by the side of the road at the Conningdale mine. Some vughs were lined with drusy quartz and occasional stibnite crystals to 20 mm. In one specimen, stibnite crystals were seen to be partly altered to kermesite and then to a cream to white secondary phase. The latter was identified as comprising approximately equal amounts of stibiconite-roméite and cervantite. In other samples of oxidised lode breccia more yellow to orange material was identified as a mixture of roméite, natrojarosite and hydronium jarosite; anhydrite, CaSO_4 , was also present in some specimens. Stibiconite-roméite was also noted as complete replacements of stibnite in quartz. Tan to brown coloured crusts lining vughs in oxidized lode breccia were found to consist solely of tripuhyite.

A similar pattern of oxidised mineral occurrence was noted at the Thalgarrah mine. White, crystalline stibiconite-roméite pseudomorphous after stibnite crystals occur in a highly weathered, quartz-rich box-work gossan. Fe-stained stibiconite-roméite surrounded this material. A vugh in gossan bearing remnant stibnite carried light brown roméite as epimorphs after rhombohedral calcite crystals.

Partially oxidised stibnite occurs in the outcrop of the Sunlight lode in Bakers Creek gorge at Hillgrove. Cream cervantite is present on the surface of the stibnite and this is coated in turn by stibiconite-roméite as the sole secondary Sb phase. A sample of white to yellow alteration product growing on oxidising stibnite was collected underground from the back of the 1740 level of the Syndicate mine at Hillgrove. XRD showed the presence of a jarosite group mineral, quartz, goethite and trace amounts of roméite and stibiconite.

At the Razorback mine near Sofala, only one secondary Sb mineral was identified and very little secondary mineralisation was present at the surface. A specimen of quartz-rich gossan carrying a considerable amount of unaltered stibnite was recovered from the dump. The specimen contained veins up to 2 mm thick of a white phase identified as stibiconite. The refined unit cell gave $a = 10.261(2) \text{ \AA}$ and SEM/EDS analysis indicated the presence of significant amounts of Ca. The sample also carried small (mm) patches of yellow, Fe-stained stibiconite that gave an identical XRD trace.

Bayley Park Geochemical Orientation Survey

Analytical results for a suite of elements for soil samples taken as part of the orientation survey are listed in Appendix 2. The only element that appears to correlate in soils with the known mineralisation is Sb.

CHAPTER 5 DISCUSSION

Solubility Phenomena

Bindheimite, $\text{Pb}_2\text{Sb}_2\text{O}_7$, roméite, $\text{Ca}_2\text{Sb}_2\text{O}_7$, bottinoite, $\text{Ni}[\text{Sb}(\text{OH})_6]_2 \cdot 6\text{H}_2\text{O}$, brandholzite, $\text{Mg}[\text{Sb}(\text{OH})_6]_2 \cdot 6\text{H}_2\text{O}$, and tripuhyite, FeSbO_4 , were chosen for study due to their relatively common occurrence in Nature or their geochemical significance. All have been synthesised here for the first time at ambient temperatures by double decomposition of aqueous solutions of component species, reflecting their real mode of formation in the oxidized zones of Sb-rich deposits.

At 25°C, the solubilities of the minerals containing the $\text{Sb}(\text{OH})_6^-$ ion follow the series mopungite > brandholzite > bottinoite, but all three have appreciable solubility. All three are substantially less soluble than the K^+ salt. This is in line with the rarity of mopungite and brandholzite (6 and 3 reported localities) and the fact that $\text{KSb}(\text{OH})_6$ has not been reported as a naturally occurring phase. Nevertheless, bottinoite is known from some 30 deposits world-wide (tabulated on mindat.org) and this at first glance may be surprising. However, this nickel antimonate mineral is invariably found as an oxidation product of ullmannite, NiSbS (Anthony *et al.*, 1990-2003; mindat.org). As ullmannite is oxidised by thin surface layers of oxygen-bearing solutions, the formation of bottinoite can be viewed as a mineralogical and geochemical inevitability (Figure 5.1). Oxidation products will ultimately be Ni^{2+} , SO_4^{2-} and $\text{Sb}(\text{OH})_5$ or $\text{Sb}(\text{OH})_6^-$ and the simultaneous generation of Ni^{2+} and $\text{Sb}(\text{OH})_6^-$ will lead to the crystallization of bottinoite due to high local concentrations of its component ions. It should be remembered that this process generally takes place in thin surface films of solution and secondary Sb sulfate minerals are very rare and probably of low stability (Anthony *et al.*, 1990-2003). It is further noted that mopungite, brandholzite and bottinoite are unstable in the presence of appreciable amounts of Ca^{2+} , a common ion in ground waters, or Pb^{2+} , present in an oxidising assemblage containing, in addition to primary Sb minerals, galena, PbS , or Pb-bearing sulfosalts. This is borne out by our measurements of the solubilities of $\text{Ca}_2\text{Sb}_2\text{O}_7$ and $\text{Pb}_2\text{Sb}_2\text{O}_7$.

As noted in the Experimental section, there is no evidence for the formation of the crystalline salts $[\text{Ca}(\text{H}_2\text{O})_6][\text{Sb}(\text{OH})_6]_2(\text{s})$ and $[\text{Pb}(\text{H}_2\text{O})_6][\text{Sb}(\text{OH})_6]_2(\text{s})$, species that would



Figure 5.1. Bottinoite (blue) altering from ullmannite (dark grey). The specimen is approximately 2 mm across (mindat.org image).

be analogous to brandholzite and bottinoite. In contrast to this, Johnson *et al.* (2005) reported in passing solubility products for both salts. At 25°C K_{SP} values of $10^{-12.55}$ and $10^{-11.02}$ were given for $\text{Ca}(\text{H}_2\text{O})_6[\text{Sb}(\text{OH})_6]_2$ and $[\text{Pb}(\text{H}_2\text{O})_6][\text{Sb}(\text{OH})_6]_2$, respectively. These correspond to respective solubilities of about 6.5×10^{-5} and $2.1 \times 10^{-4} \text{ mol dm}^{-3}$, indicating that they are reasonably soluble phases. It can only be concluded that these quantities refer in fact to the upper limits of the solubilities of the X-ray amorphous phases, corresponding to dissolved Sb levels of 10 ppm for the Ca salt and 32 ppm for the Pb salt. If this were the case, the conclusion that Sb is relatively mobile in the supergene zone would be logical. The solubility experiments described here, however, render such a conclusion untenable.

At 25°C, $\text{Pb}_2\text{Sb}_2\text{O}_7$ equilibrated with 0.0100 M HNO_3 gave a final pH of 2.05, total dissolved Pb equal to $4.12 \times 10^{-5} \text{ mol dm}^{-3}$ (ca 8.5 ppm) and total dissolved Sb equal to $7.7 \times 10^{-8} \text{ mol dm}^{-3}$ (ca 9.3 ppb). Similarly, $\text{Ca}_2\text{Sb}_2\text{O}_7$ equilibrated with 0.0100 M HNO_3 gave a final pH of 2.23, total dissolved Ca equal to $2.115 \times 10^{-3} \text{ mol dm}^{-3}$ (ca 85 ppm) and total dissolved Sb equal to $3.3 \times 10^{-7} \text{ mol dm}^{-3}$ (ca 40 ppb). It is evident that it is more difficult to remove Pb from the bindheimite lattice than Ca from roméite. This and the above results reflect the facts that the salts act as cation exchangers (England *et al.*, 1980; Baetsle and Huys, 1968; Riviere *et al.*, 1988; Slade *et al.*, 1996 and references therein) and dissolve incongruently. Most significantly, dissolved Sb concentrations are about three orders of magnitude smaller than those predicted by Johnson *et al.* (2005). Stibiconite group minerals are very effective in immobilising Sb in the oxidised environment and

stibiconite group minerals are very common in the vicinity of oxidising Sb ore deposits. Thus the commonly perceived wisdom that Sb is mobile in the supergene zone as a result of chemical dispersion is in error. This is exactly what was anticipated in that previous suppositions on the matter rested on the erroneous assumption that $\text{Sb}_2\text{O}_5(\text{s})$ could be used as a proxy for modelling the solution behaviour of Sb(V) in the oxidised environment.

Secondary Mineral Assemblages

The above predictions made on the basis of solubility experiments are reinforced by what is known in terms of mineral assemblages and relationships in the oxidised zones of Sb-bearing ore bodies. Only a handful of secondary Sb minerals occur commonly and these are kermesite, the dimorphs valentinite and sénarmontite, cervantite, tripuhyite, and three members of the stibiconite group, bindheimite, roméite and stibiconite (Anthony *et al.*, 1990-2003). It is remarkable that the oxidation of stibnite, Sb_2S_3 , always leads to assemblages of these common minerals in the *immediate* proximity of their primary precursors and pseudomorphs of them after stibnite are very common (*c.f.*, Figure 5.2).



Figure 5.2. Stibiconite after stibnite, Real de Catorce, San Luis Potosí, Mexico: Field of view 6x4 cm. Photo: Malcolm Tiddy. Specimen: P.A. Williams.

With respect to field studies carried out in conjunction with the solubility work, the secondary Sb mineralogy of the Bayley Park prospect, the Conningdale mine, the Thalgarrah mine and the Syndicate and Sunlight lodes in the Hillgrove area of New South Wales (Gilligan *et al.*, 1992) and the Razorback mine near Mudgee, New South Wales (Staude, 1970) has been characterised. In all cases primary Sb mineralisation consists of stibnite. Kermesite pseudomorphs after stibnite were observed at the Conningdale mine. Otherwise, small amounts of sénarmontite and cervantite were found coating the surface of

partially altered stibnite and overlying this were layers and crusts of stibiconite group minerals (stibiconite and roméite); the latter also formed pseudomorphs after stibnite in some specimens. Adjacent to these minerals small wart-like masses of brown tripuhyite were identified by XRD at the Conningdale mine and the Bayley Park prospect. The extent of migration of the bulk of the Sb in these deposits can be measured in millimetres and mineral occurrences and paragenesis are consistent both with the solubility results described above and the progressive oxidation of Sb(III) to Sb(V). To further emphasise this point, attention is drawn to Figure 5.3. The picture is of the lode outcrop, *exposed at surface*, of Fishers Antimony mine, near Hillgrove.



Figure 5.3. Stibnite (grey) altering to stibiconite (cream) immediately to the right of the hand lens, Fishers antimony mine, Hillgrove, New South Wales. Photo: P.A. Williams

The photograph shows stibnite altering to stibiconite at the entrance of the upper adit driven on the lode. The deposit has been weathering at least since the last glaciation (*ca* 15 Ka) and the extent of chemical migration of Sb is obviously negligible.

Bayley Park Geochemical Orientation Survey

In light of the conclusion that Sb is in fact quite immobile in the weathering environment, a soil geochemistry orientation survey was conducted over the Bayley Park prospect on the tablelands out of the gorge area (AGM 55 grid reference 56J 03914E 66244N) This was part of a validation of predictions concerning the use of soil Sb analyses in the exploration context. The prospect occurs in gently sloping country and is comparatively free of

contamination by earlier mining operations. The sole workings over a 500 m strike length consist of an old back-filled shaft, a prospecting shaft some 15 m deep dating from 1971 and a few shallow (0.5 m) prospecting pits. Costeans put in to test the deposit in 1971 cannot be traced and the extent of contamination of soils at the site is very limited as virtually no mining or ore treatment has taken place. Mineralization is hosted in a sub-vertical fault filled with brecciated metasediments and stibnite cemented by quartz. Arsenopyrite is reported to be present in the primary ore (Gilligan *et al.*, 1992) but none was found in the field. Soil cover is thin, typically less than 0.2 m. Three parallel sampling traverses perpendicular to the mineralised shear were surveyed and soil samples from the B horizon taken along them at 20 m intervals. Care was taken to locate the sample sites well clear of the low level contamination associated with low dumps (< 0.2 m high) near the two shafts. Assay results are given in Appendix 2. Plotting the results showed that there was no apparent correlation between the position of the mineralised shear and any of the elements analysed, except for Sb. This is certainly true for As and the fact that soil assays for the element show no relation to the mineralisation is consistent with the fact that As is much more mobile than Sb, as exemplified by numerous field studies (Hawkes and Webb, 1962; Rose *et al.*, 1979).

A contoured plot of the Bayley Park soil geochemistry Sb results with 20 ppm interval contour lines is shown in Figure 5.4. In the Figure, the positions of older prospecting pits and shafts are indicated by crosses and Sb assays (ppm) are shown in red. The trend of these workings delineates for all practical purposes the trend of the shear hosting the stibnite and arsenopyrite mineralisation. Anomalous Sb values are closely associated with the shear.

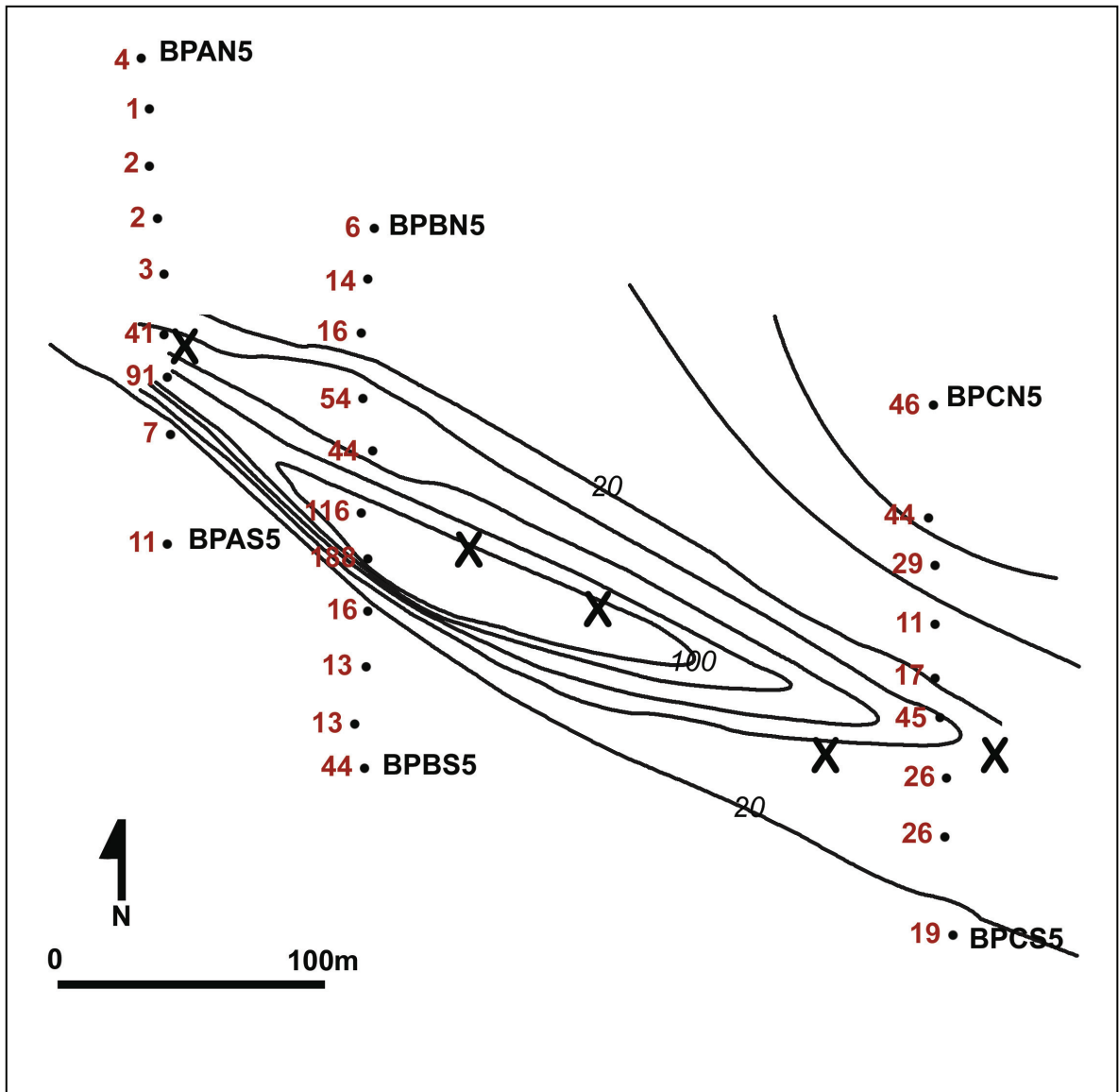


Figure 5.4. Bayley Park soil geochemistry Sb results with 20 ppm contour interval.

Sb dispersion away from the lode is not extensive. The geochemical soil anomaly associated with the deposit shear zone reached Sb levels of about 190 ppm and delineated the NW–SE shear zone perfectly. Of particular interest was the fact that soil Sb levels had dropped to about 10 ppm within 50 m of the known mineralisation and reached background levels (*circa* 4–8ppm; see Hillgrove Sb histogram, Figure 5.5) within about another 50 m. Several assays returned <4 ppm.

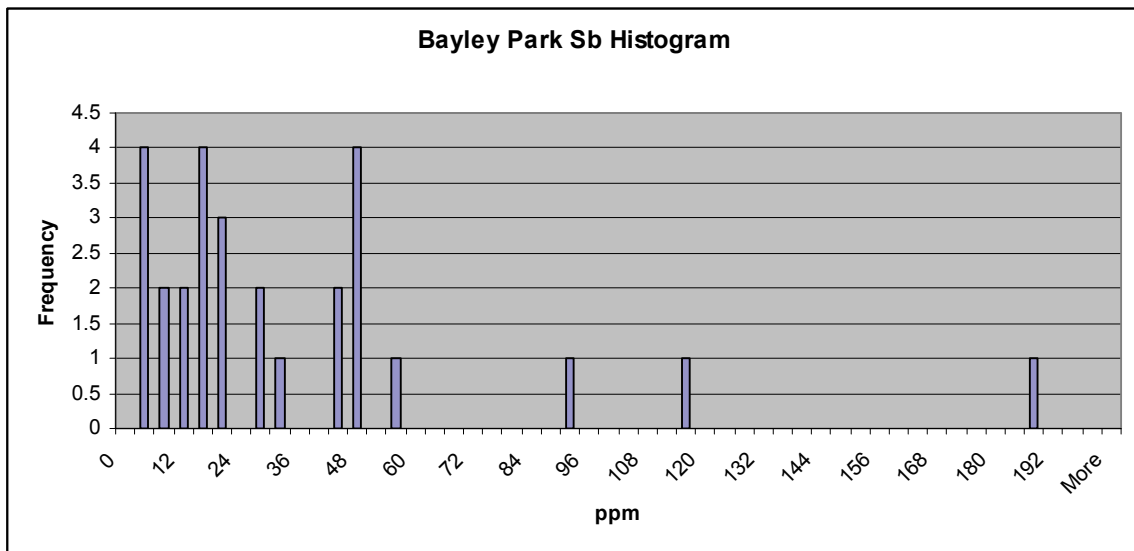


Figure 5.5. Frequency histogram for Bayley Park Sb soil data.

The orientation survey clearly showed that anomalous Sb levels are confined to the immediate vicinity of the oxidising lode and are consistent with the view of Wilson *et al.* (2004) that the chemical mobility of Sb in soils is quite limited. It is thus concluded that the use of Sb in geochemical exploration in the area is useful to pin point potentially mineralised zones. This close grid style of sampling for Sb may be very useful to identify the location and orientation of drill targets for this ‘hit or miss’ style of thin sub-vertical shear mineralisation that commonly occurs throughout the New England region of New South Wales. Nevertheless, this method of soil sampling would not be economic on a regional scale and this points to the necessity for cheaper exploration options, including detailed geological mapping and rock chip sampling.

Furthermore, the orientation study, resting on the solubility experiments described earlier, suggests that Sb is probably of little use as a pathfinder element in regional geochemical surveys. The expression of Sb anomalies may be very subtle, if at all detectable, for regional soil data. Therefore it will be much more effective to use other geochemical pathfinder elements for locating Sb ore deposits.

CONCLUDING COMMENTS

This Honours research topic has combined solubility experiments involving certain known secondary mineral phases in an effort to assess the chemical mobility of Sb in solution. It has been concluded that, contrary to previously published assertions on the matter, the element is essentially immobilised in common Sb(V) phases and that it should have limited chemical mobility in soils or natural aqueous solutions. This, in turn, serves to rationalise many observations concerning the close association of secondary Sb minerals with their primary precursors world-wide. Such associations have been re-emphasised by a brief survey of similar mineralisation in a number of deposits in New South Wales. Based on these studies, a scoping orientation geochemical survey was carried out over known Sb mineralisation. The conclusions reached in the laboratory study were completely vindicated and a useful geochemical tool for pin pointing Sb-rich mineralisation using soil sampling methods has been developed. The chemical-mineralogical-geochemical approach adopted appears to be a powerful one, and one which might be profitably explored for other elements.

Finally, it is pleasing to note that the results of this investigation have been incorporated in the exploration strategy of Straits Hillgrove Gold Ltd.

REFERENCES

- Abe, M. (1979) Synthetic inorganic ion-exchange materials. XX. Ion-exchange properties of crystalline antimonite(V) acid with alkaline earth metal ions. *Bulletin of the Chemical Society of Japan*, **52**, 1386-1390.
- Accornero, M., Marini, L. and Lelli, M. (2008) The Dissociation constant of antimonite acid at 10-40°C. *Journal of Solution Chemistry*, **37**, 785-800.
- Aylward, G. and Findlay, T. (2002) *SI Chemical Data, 5th Edition*. John Wiley & Sons Australia.
- Anon. (1988) Concordia/Siegerland. *Emser Hefte*, 19-29.
- Anthony, J.W., Bideaux, R.A., Bladh, K.W. and Nichols, M.C. (1990-2003) *Handbook of Mineralogy*. Volumes I-V, Mineral Data Publishing, Tucson.
- Appelo, C.A.J. and Postma, D. (1993) *Geochemistry, Groundwater and Pollution*. Balkema, Rotterdam.
- Arents, A. (1867), Partzite, a new mineral. *American Journal of Science, series 2*, **43**, 362.
- Ashley, P.M. and Craw, D. (2004) Structural controls on hydrothermal alteration and gold-antimony mineralisation in the Hillgrove area, NSW, Australia. *Mineralium Deposita*, **39**, 223-239.
- Ashley, P.M., Cook, N.D.J., Hill, R.L. and Kent, A.J.R. (1993) Lamprophyre dykes and their relation to mesothermal Au-Sb veins at Hillgrove, Southern New England Orogen, New South Wales. *New England Orogen, Eastern Australia Symposium*, University of New England, Armidale, pp. 359-375.
- Babčan, J. (1976) Entstehung und Stabilität von Antimonmineralen im System Sb^{3+} - S^{2-} - H^+ - OH^- . *Chemie der Erde*, **35**, 281-284.
- Baes, C.F., Jr and Mesmer, R.E. (1976) *The Hydrolysis of Cations*. Wiley Interscience, New York.
- Baetsle, L.H. and Huys, D. (1968) Structure and ion exchange characteristics of polyantimonite acid. *Journal of Inorganic and Nuclear Chemistry*, **30**, 639-649.
- Basso, R., Cabella, R., Lucchetti, G., Marescotti, P. and Martinelli, A. (2003) Structural studies on synthetic and natural Fe-Sb-oxides of MO_2 type. *Neues Jahrbuch für Mineralogie, Monatshefte*, 407-420.
- Basso, R., Lucchetti, G., Zefiro, L. and Palenzona, A. (1999) Clinocervantite, β - Sb_2O_4 , the natural monoclinic polymorph of cervantite from the Cetine mine, Siena, Italy. *European Journal of Mineralogy*, **11**, 95-100.
- Beintema, J. (1936) On the crystal structure of magnesium- and nickel antimonite. *Proceedings of the Royal Academy of Sciences of Amsterdam*, **39**, 241-252.
- Belevantsev, V.I., Gushchina, L.I. and Obolenskii A.A. (1998) Antimony in hydrothermal solutions: analysis and generalization of data on antimony(III) chloride complexes. *Geochemistry International*, **36**, 928-933.
- Berbain, C. and Favreau, G. (2007) Un exemple peu courant de minéralisation nickélique: le Correc d'en Llinassos à Oms (Pyrénées-Orientales). *Le Cahier des Micromonteurs*, **95**, 3-24.
- Berlepsch, P., Armbruster, T., Brugger, J., Criddle, A.J. and Graeser, S. (2003) Tripuhyite, FeSbO_4 , revisited. *Mineralogical Magazine*, **67**, 31-46.
- Blandamer, M.J., Burgess, J. and Peacock, R.D. (1974) Solubility of sodium hexahydroxoantimonate in water and in mixed aqueous solvents. *Journal of the Chemical Society, Dalton Transactions*, 1084-1086.
- Bonazzi, P., Menchetti, S. and Sabelli, C. (1987) Structure refinement of kermesite: symmetry, twinning, and comparison with stibnite. *Neues Jahrbuch für Mineralogie, Monatshefte*, 557-567.

- Bonazzi, P., Menchetti, S., Caneschi, A. and Magnanelli, S. (1992) Bottinoite, $\text{Ni}(\text{H}_2\text{O})_6[\text{Sb}(\text{OH})_6]_2$, a new mineral from the Bottino mine, Alpi Apuane, Italy. *American Mineralogist*, **77**, 1301-1304.
- Borovikov, A.A., Gushchina, L.V., Shebanin, A.P. and Pavlova, G.G. (2005) Complexation of antimony(III) in chloride-rich acidic solutions at temperatures of 20-200°C: A Raman spectroscopic study and thermodynamic modelling. *Geochemistry International*, **43**, 1024-1027.
- Bothwell, D.I., Davis, R.J. and Moss, A.A. (1960) A bismuth-bearing variety of bindheimite. *Mineralogical Magazine*, **32**, 664-666.
- Brisse, F., Stewart, D.J., Seidl, V. and Knop, O. (1972) Pyrochlores. VIII. Studies of some 2-5 pyrochlores and related compounds and minerals. *Canadian Journal of Chemistry*, **50**, 3648-3666.
- Brookins, D.G. (1986) Geochemical behaviour of antimony, arsenic, cadmium and thallium: Eh-pH diagrams for 25°C, 1-bar pressure. *Chemical Geology*, **54**, 271-278.
- Brugger, J., Gieré, R., Graeser, S. and Meisser, N. (1997) The crystal chemistry of roméite. *Contributions to Mineralogy and Petrology*, **127**, 136-146.
- Bryndzia, L.T. and Kleppa, O.J. (1988) High temperature reaction calorimetry of solid and liquid phases in part of the quasi-binary system $\text{Cu}_2\text{S}-\text{Sb}_2\text{S}_3$. *American Mineralogist*, **73**, 707-713.
- Buschmann, J., Canonica, S. and Sigg, L. (2005) Photoinduced oxidation of antimony (III) in the presence of humic acid. *Environmental Science & Technology*, **39**, 5335-5341.
- Byström, A., Hök, B. and Mason, B. (1941) The crystal structure of zinc metantimonate and similar compounds. *Arkiv för Kemi, Mineralogi och Geologi*, **15B**, 1-8.
- Carne, J.E. (1903) Report on the Razorback gold and antimony mine. Annual Reports of the NSW Department of Mines for 1902, pp. 124-125.
- Casas, J.M., Crisóstomo, G. and Cifuentes, L. (2004) Antimony solubility and speciation in aqueous sulphuric acid solutions at 298 K. *Canadian Journal of Chemical Engineering*, **82**, 175-183.
- Clark, A. M. (1993) Bottinoite, a mineral new to Britain. *Mineralogical Magazine*, **57**, 543-544.
- Clarke, I. and Raphael, N. (1982) A resource evaluation of the Razorback gold-antimony mine. Geological Survey of New South Wales, Department of Mineral Resources.
- Comsti, E.C. and Taylor, G.R. (1984) Implications of fluid inclusion data on the origin of the Hillgrove gold-antimony deposits, N.S.W. *Proceedings of the Australasian Institute of Mining and Metallurgy*, **289**, 195-203.
- Dehlinger, U. (1928) Über die Kristallstruktur der Antimonoxyde. *Zeitschrift für Kristallographie*, **66**, 108-119.
- Dehlinger, U. and Glocker, R. (1927) Über den atomaren Aufbau der Antimonoxyde. *Zeitschrift für anorganische und allgemeine Chemie*, **165**, 41-45.
- Dihlström, K. and Westgren, A. (1937) Über den Bau des sogenannten Antimontetroxyds und der damit isomorphen Verbindung $\text{BiTa}_2\text{O}_6\text{F}$. *Zeitschrift für anorganische und allgemeine Chemie*, **235**, 153-160.
- Dunning, G.E. and Cooper, J.F., Jr. (2005) Mineralogy of the Spring Creek area, Last Chance mining district, Plumas County, California. *Axis*, **1**, 1-30.
- England, W.A., Cross, M.G., Hamnett, A., Wiseman, P.J. and Goodenough, J.B. (1980) Fast proton conduction in inorganic ion-exchange compounds. *Solid State Ionics*, **1**, 231-249.
- Ertl, A. and Brandstätter, F. (2000) Protopartzite or thrombolite from magnesite quarry Veitsch, Sattlerkogel, Styria, Austria. *Joannea – Mineralogie*, **1**, 27-30.
- Filella, M. and May, P.M. (2003) Computer simulation of the low-molecular-weight inorganic species distribution of antimony(III) and antimony(V) in natural waters. *Geochimica et Cosmochimica Acta*, **67**, 4013-4031.

- Filella, M., Belzile, N. and Chen, Y.-W. (2002a) Antimony in the environment: a review focused on natural waters I. Occurrence. *Earth-Science Reviews*, **57**, 125-176.
- Filella, M., Belzile, N. and Chen, Y.-W. (2002b) Antimony in the environment: a review focused on natural waters II. Relevant solution chemistry. *Earth-Science Reviews*, **59**, 265-285
- Friedrich, A., Mazzi, F. Wildner, M. and Tillmanns, E. (2003) Addendum: Isotypism of $\text{Co}(\text{H}_2\text{O})_6[\text{Sb}(\text{OH})_6]_2$ with brandholzite and bottinoite. *American Mineralogist*, **88**, 462-463.
- Friedrich, A., Wildner, M., Tillmanns, E. and Merz, P.L. (2000) Crystal chemistry of the new mineral brandholzite, $\text{M}^{2+}(\text{H}_2\text{O})_6[\text{Sb}(\text{OH})_6]_2$, and of the synthetic analogues $\text{Mg}(\text{H}_2\text{O})_6[\text{Sb}(\text{OH})_6]_2$ ($\text{M}^{2+} = \text{Mg}, \text{Co}$). *American Mineralogist*, **85**, 593-599.
- Gasperin, M. (1955) Synthèse et identification de deux oxydes doubles de tantale et d'étain. *Comptes Rendus des séances hebdomadaires de l'Académie des sciences*, **240**, 2340-2342.
- Gayer, K.H. and Garrett, A.B. (1952) The equilibria of antimonous oxide (rhombic) in dilute solutions of hydrochloric acid and sodium hydroxide at 25°C. *Journal of the American Chemical Society*, **74**, 2353-2354.
- Gilligan, L.B., Brownlow, J.W., Cameron, R.G. and Henley, H.F. (1992) Dorrigo - Coffs Harbour 1:250,000 Metallogenic Map SH/56-10, SH/56-11: Metallogenic Study and Mineral Data Sheets. New South Wales Geological Survey, Sydney.
- Green, D.I., McCallum, D. and Wood, M. (2000). The Brownley Hill mine, Alston Moor district, Cumbria, England. *Mineralogical Record*, **31**, 231-250.
- Grube, G. and Schweigardt, F. (1923) Über das elektrochemische Verhalten von Wismut und Antimon in alkalischer Lösung. *Zeitschrift für Elektrochemie und angewandte physikalische Chemie*, **29**, 257-264.
- Hall, R.M. (1972) Anglo Range N.L. Report on Exploration activities. For As to E 6997 & 6998 and PLLA 492, Armidale.
- Hawkes, H.E. and Webb, J.S. (1962) Geochemistry in Mineral Exploration. Harper and Row, New York.
- Hussak, E. and Prior, G.T. (1897) On tripuhyite, a new antimonite of iron, from Tripuhy, Brazil. *Mineralogical Magazine*, **11**, 302-303.
- Jain, D.V.S. and Banerjee, A.K. (1961) On the structure of antimonates. *Journal of Inorganic and Nuclear Chemistry*, **19**, 177-179.
- Jander, G. and Brüll, W. (1926) Über amphotere Oxydhydrate, deren wässrige Lösungen und kristallisierte Salze. IV. Mitteilung: Über die Antimonsäuren und die Alkaliantimonate. *Zeitschrift für anorganische und allgemeine Chemie*, **158**, 321-342.
- Jansen, M. (1978) Darstellung und Kristallstruktur von $\text{Sb}_2\text{O}_5 \cdot 3/5\text{H}_2\text{O} = \text{Sb}_5\text{O}_{12}(\text{OH}) \cdot \text{H}_2\text{O}$. *Revue de Chimie Minérale*, **15**, 242-247.
- Jansen, M. (1979a) Über eine neue Modifikation von As_2O_5 . *Zeitschrift für Naturforschung*, **34b**, 10-13.
- Jansen, M. (1979b) Die Kristallstruktur von Antimon(V)-oxid. *Acta Crystallographica*, **B35**, 539-542.
- Johnson, C.A., Moench, H., Wersin, P., Kugler, P. and Wenger, C. (2005) Solubility of antimony and other elements in samples taken from shooting ranges. *Journal of Environmental quality*, **34**, 248-254.
- Kang, S.-Q., Zheng, D.-J. and Fu, C.-Y. (1992). Fundamental studies on the hydrometallurgy of antimony equilibria of $\text{Sb}_2\text{S}_3\text{-Cl-H}_2\text{O}$ system. *Proceedings of the Second International Conference on Hydrometallurgy*, pp. 112-115. International Academic Publishers, Beijing.
- Kol'tsova, T.N. and Chastukhin, A.E. (2002) Phase relations in the Cu-Sb-O system. *Inorganic Materials*, **38**, 1228-1234.

- Konopik, N. and Zwiauer, J. (1952) Über Antimontetroxid. *Monatshefte für Chemie*, **83**, 189-196.
- Koritnig, S. (1967) Der Thrombolith von der Veitsch, Steiermark. *Mitteilungen der Abteilung für Bergbau, Geologie und Paläontologie des Landesmuseums Joanneum*, **1-2**, 51-56.
- Krupka, K.M. and Serne, R.J. (2002) Geochemical factors affecting the behaviour of antimony, cobalt, europium, technetium, and uranium in vadose sediments. *United States Department of Energy Pacific Northwest Laboratory Report*, PNNL-14126.
- Kupcik, V. (1967) Die Kristallstruktur des Kermesits, $\text{Sb}_2\text{S}_2\text{O}$. *Naturwissenschaften*, **54**, 114.
- Lancashire, R.J. (1995) Windows version of COMICS. Available at wwwchem.uwimona.edu.jm:1104/software/comics.html.
- Langford, J.I. (1973) Least-squares refinement of cell dimensions from powder data by Cohen's method. *Journal of Applied Crystallography*, **6**, 190-196.
- Lefebvre, J. and Maria, H. (1963) Étude des équilibres dans les solutions récentes de polyantimoniates. *Comptes rendus de l'Académie des sciences de Paris*, **256**, 3121-3124.
- Leuz, A.K., Mönch, H. and Johnson, C. A. (2006) Sorption of Sb(III) and Sb(V) to goethite: influence on Sb(III) oxidation and mobilization. *Environmental Science Technology*, **40**, 7277-7282.
- Lumpkin, G.R. and Ewing, R.C. (1992) Geochemical alteration of pyrochlore minerals: microlite subgroup. *American Mineralogist*, **77**, 179-188.
- Mason, B. and Vitaliano, C.J. (1953) The mineralogy of the antimony oxides and antimonates. *Mineralogical Magazine*, **30**, 100-112.
- Massalski, T., Ed. (1990) *Binary Alloy Phase Diagrams*. ASM International, Materials Park, Ohio, second edition.
- Mishra, S.K. and Gupta, Y.K. (1968) Spectrophotometric study of the hydrolytic equilibria of Sb(III) in aqueous perchloric acid solution, *Indian Journal Chemistry*, **6**, 757-758.
- Mitsunobu, S., Harada, T. and Takahashi, Y. (2006) Comparison of antimony behaviour with that of arsenic under various soils redox conditions. *Environmental Science and Technology*, **40**, 7270-7276.
- Nakai, I. and Appleman, D.E. (1980) klebelsbergite, $\text{Sb}_4\text{O}_4(\text{OH})_2\text{SO}_4$: redefinition and synthesis. *American Mineralogist*, **65**, 499-505.
- Nakua, A., Yun, H., Reimers, J.N., Greedan, J.E. and Stager, C.V. (1991) Crystal structure, short range and long range magnetic ordering in CuSb_2O_6 . *Journal of Solid State Chemistry*, **91**, 105-112.
- Natta, G. and Baccaredda, M. (1933) Tetrossido di antimonio e antimoniati. Struttura cristallina dell' antimoniato di antimonile (tetrossido di antimonio), suo isomorfismo con i piroantimoniati di piombo e di calcio ed esame röntgenografico delle ocre di antimonio (Cervantite, Stibiconite) e degli antimoniati idrati di calcio (Idroromeite) e di piombo (Bindheimite). *Zeitschrift für Kristallographie*, **85**, 271-296.
- Neumann, H.M. (1954) Antimony(V) species in hydrochloric acid solution. *Journal of the American Chemical Society*, **76**, 2611-2615.
- Nishimura, T. and Tozawa, K. (1986) Behavior of antimony and arsenic in sulfuric acid solution. *Metallurgical Review of the Mining and Metallurgical Institute of Japan*, **3(2)**, 131-145.
- Orosel, D. (2007) *Untersuchung von Druckumwandlungen an Oxiden und Fluoriden und Synthese neuer Verbindungen*. Dissertation, Max-Planck-Institut für Festkörperforschung, Stuttgart, Germany.
- Palenik, R.C., Abboud, K.A. and Palenik, G.J. (2005) Bond valence sums and structural studies of antimony complexes containing Sb bonded only to O atoms. *Inorganica Chimica Acta*, **358**, 1034-1040.

- Pankajavalli, R. and Sreedharan, O.M. (1987) Thermodynamic stability of Sb_2O_4 by a solid oxide electrolyte e.m.f. method. *Journal of Materials Science*, **22**, 177-180.
- Pantani, F. and Desideri, P.G. (1959) Il comportamento polarografico dell'antimonio(III) in soluzione cloridiche. *Gazzetta Chimica Italiana*, **89**, 1360-1372.
- Past, V. (1985) Antimony. In: Bard, A.J., Parsons, R. and Jordan, J. (Eds) *Standard Potentials in Aqueous Solution*. Marcel Dekker, New York, pp. 172-179.
- Pawlowski, D. (1991) *Mineralfundstellen im Sauerland*. Weise, Munich.
- Perrin, D.D. and Sayce, I.G. (1967) Computer calculation of equilibrium concentrations in mixtures of metal ions and complexing species. *Talanta*, **14**, 833-842.
- Pilarski, J., Waller, P. and Pickering, W. (1995) Sorption of antimony species by humic acid. *Water, Air, and Soil Pollution*, **84**, 51-59.
- Pitman, A.L., Pourbaix, M. and de Zoubov, N. (1957) Comportement électrochimique de l'antimoine. *Rapport Technique Cebelcor*, **50**, Report No. 55.
- Plimer, I.R. (1982) Minerals of the Consols mine and mine sequence. In: Worner, H.K. and Mitchell, R.W. (Eds), *Minerals of Broken Hill*. Australian Mining and Smelting Limited, Melbourne, pp. 66-67.
- Pokrovski, G.S., Borisova, Y.B., Roux, J., Hazemann, J.-L., Petdang, A., Tella, M. and Testemale, D. (2006) Antimony speciation in saline hydrothermal fluids: a combined X-ray absorption fine structure spectroscopy and solubility study. *Geochimica et Cosmochimica Acta*, **70**, 4196-4214.
- Ransome, A.L. (1940) General geology and the ores of the Blind Spring Hill mining district, Mono County, California. *Californian Journal of Mines and Geology*, **36**, 159-197.
- Riviere, M., Fourquet, J.L., Grins, J. and Nygren, M. (1988) The cubic pyrochlores $\text{H}_{2x}\text{Sb}_{2x}\text{W}_{2-2x}\text{O}_6 \cdot n\text{H}_2\text{O}$; structural, thermal and electrical properties. *Materials Research Bulletin*, **23**, 965-975.
- Robie, R.A. and Hemmingway, B.S. (1995) Thermodynamic properties of minerals and related substances at 298.15 K and 1 bar (10^5 Pascals) pressure and at higher temperatures. *US Geological Survey Bulletin*, **2131**.
- Rose, A.W., Hawkes, H.E. and Webb, J.S. (1979) *Geochemistry in Mineral Exploration*. Academic Press, London.
- Ryzhenko, B.N., Shapkin, A.I. and Bryzgalin, O.V. (1985) Electrolytic dissociation of metal sulfates in water solution. *Geochemistry International*, **22**, 5-11.
- Schrewelius, N. (1938) Röntgenuntersuchung der Verbindung $\text{NaSb}(\text{OH})_6$, NaSbF_6 , NaSbO_3 , und gleichartiger Stoffe. *Zeitschrift für anorganische und allgemeine Chemie*, **238**, 241-254.
- Schuhmann R. (1924) The free energy of antimony trioxide and the reduction potential of antimony. *Journal of the American Chemical Society*, **46**, 52-58.
- Schulze, H. (1883) Antimontrisulfid in wässriger Lösung. *Journal für praktische Chemie*, **27**, 320-332.
- Seal, R.R., II, Robie, R.A., Hemmingway, B.S. and Barton, P.B., Jr (1992) Superambient heat capacities of synthetic stibnite, berthierite and chalcostibite: revised thermodynamic properties and implications for phase equilibria. *Economic Geology*, **87**, 1911-1918.
- Shimada, S. and Ishii, T. (1989) An alternative route to copper antimony oxide, $\text{Cu}_9\text{Sb}_4\text{O}_{19}$. *Reactivity of Solids*, **7**, 183-186.
- Shimada, S. and Mackenzie, K.J.D. (1982) Solid-state reactions in the system Cu-Sb-O; formation of a new copper(I) antimony oxide. *Thermochimica Acta*, **56**, 73-82.
- Shimada, S., Kodaira, K. and Matsushita, T. (1985) Preparation and characterization of a new copper antimony oxide, $\text{Cu}_9\text{Sb}_4\text{O}_{19}$. *Journal of Solid State Chemistry*, **59**, 237-241.

- Shimada, S., Mackenzie, K.J.D., Kodaira, K., Matsushita, T. And Ishii, T. (1988) Formation of new copper antimony oxides by solid state reaction between CuSb_2O_6 and CuO under atmospheric and high pressure. *Thermochimica Acta*, **133**, 73-77.
- Simpson, C. (2007) Straits Hillgrove Gold Pty Ltd, Hillgrove NSW Annual Report for the period 23/08/2006 to 22/08/2007 (Confidential).
- Slade, R.C.T., Hall, G.P., Ramanan, A. and Prince, E. (1996) Structure and proton conduction in pyrochlore-type antimonite acid: a neutron diffraction study. *Solid State Ionics*, **92**, 171-181.
- Sleight, A.W. (1969) AgSbO_3 : chemical characterization and structural considerations. *Materials Research Bulletin*, **4**, 377-380.
- Smith, G. (1922) Notes on the mineralogy of the Broken Hill district. *Memoirs of the Geological Survey of New South Wales*, **8**, 403-416.
- Smith R.M., Martell. A.E. (1976) *Critical Stability Constants. Volume 4. Inorganic Complexes*, Plenum Press, New York.
- SRL, Straits Resources Limited - ASX Preliminary final report, 30 June 2008, Lodged with the ASX 01/09/2008.
- Staude, W.J. (1970) The Razorback mine near Sofala, New South Wales. Geological Survey of New South Wales, *Rep. GS1970/188*, Department of Mines.
- Steely, S., Amarasiriwardena, D. and Xing, B. (2007) An investigation of inorganic antimony species and antimony associated with soil humic acid molar mass fractions in contaminated soils. *Environmental Pollution*, **148**, 2, 590-598.
- Stewart, D.J. and Knop, O. (1970) Pyrochlores. VI. Preparative chemistry of sodium and silver antimonates and related compounds. *Canadian Journal of Chemistry*, **48**, 1323-1332.
- Swaminathan, K. and Sreedharan, O.M. (2003) High temperature stabilities of interoxides in the system Fe-Sb-O and their comparison with the interoxides in other M-Sb-O (M = Cr, Ni or Co) systems. *Journal of Alloys and Compounds*, **358**, 48-55.
- Thanabalasingam, P. and Pickering, W.F. (1990) Specific sorption of antimony (III) by the hydrous oxides of Mn, Fe, and Al. *Air, water, and soil pollution*, **49**, 175-185.
- Tighe, M., Lockwood, P. and Wilson, S. (2005) Absorption of antimony(V) by floodplain soils, amorphous iron(III) hydroxide and humic acid. *Journal of Environmental Monitoring*, **7**, 1177-1185.
- Tourky, A.R. and Mousa, A.A. (1948) Studies on some metal electrodes. Part V. The amphoteric properties of antimony tri- and pentoxide. *Journal of the Chemical Society*, 759-763.
- Viñals, J. and Calvo, M. (2006) Lanzuela. Teruel, Spain. Ullmanite, bottinoite and polydydimite. *Mineral Up*, **1**, 58.
- Vink, B.W. (1996) Stability relations of antimony and arsenic compounds in the light of revised and extended Eh-pH diagrams. *Chemical Geology*, **130**, 21-30.
- Vitaliano, C.J. and Mason, B. (1952) Stibiconite and cervantite. *American Mineralogist*, **37**, 982-999.
- Wagman, D.D., Evans, W.H., Parker, V.B., Schumm, R.H., Halow, I., Bailey, S.M., Churney, K.I. and Nuttall, R.I., (1982) The NBS tables of chemical thermodynamic properties: selected values for inorganic and C_1 and C_2 organic substances in SI units. *Journal of Physical and Chemical Reference Data*, **11**, Supplement Number 2.
- Walenta, K. (1983) Bismutostibiconit, ein neues Mineral der Stibiconitgruppe aus dem Schwarzwald. *Chemie der Erde*, **42**, 77-81.
- Weiss, S. (1990) *Mineralfundstellen, Deutschland West*. Weise, Munich.
- Williams, S.A. (1985) Mopungite, a new mineral from Nevada. *Mineralogical Record*, **16**, 73-74.
- Williams. P.A. (1990) *Oxide Zone Geochemistry*, Ellis Horwood, Chichester.

- Williams-Jones, A.E. and Normand, C. (1997) Controls on mineral parageneses in the system Fe-Sb-S-O, *Economic Geology*, **92**, 308-324.
- Wilson, N.J., Craw, D. and Hunter, K. (2004) Antimony distribution and environmental mobility at an historic antimony smelter site, New Zealand. *Environmental Pollution*, **129**, 257-266.
- Wittern, A. (2001) *Mineralfundorte in Deutschland*. E. Schweizerbart'sche Verlagsbuchhandlung, Stuttgart.
- Zakaznova-Herzog, V.P. and Seward, T.M. (2006) Antimonous acid protonation/deprotonation equilibria in hydrothermal solutions to 300°C. *Geochimica et Cosmochimica Acta*, **70**, 2298-2310.
- Zedlitz, O. (1932) Die Kristallstruktur von Romeit und Schneebergit. *Zeitschrift für Kristallographie*, **81**, 253-263.
- Zotov, A.V., Shikina, N.D. and Akinfiyev, N.N. (2003) Thermodynamic properties of the Sb(III) hydroxide complex $\text{Sb}(\text{OH})_3(\text{aq})$ at hydrothermal conditions. *Geochimica et Cosmochimica Acta*, **67**, 1821-1836.
- Zubkova, N.V., Pushcharovsky, D.Y., Atencio, D., Arakcheeva, A.V. and Matioli, P.A. (2000) The crystal structure of lewisite, $(\text{Ca}, \text{Sb}^{3+}, \text{Fe}^{3+}, \text{Al}, \text{Na}, \text{Mn}, \square) (\text{Sb}^{5+}, \text{Ti})_2\text{O}_6(\text{OH})$. *Journal of Alloys and Compounds*, **296**, 75-79.

APPENDIX 1

Microprobe data for the unnamed pyrochlore mineral from the Consols mine, Broken Hill

(analyses by Ian Graham, the University of New South Wales).

Analysis No.	1	3	4	6	7	7a	7c	7d
Si	1.7	1.74	1.53	1.42	1.6	0.5	0.38	0.22
S	0.05	0.02	0.04	0.05	0.03	0.05	0.06	0.03
Cl	0.39	0.05	1.7	1.79	0.05	0.02	0	0.02
Fe	1.09	1.22	1.25	1.2	1.11	17.78	20.65	25.34
Ag	0.28	0.13	5.77	11.03	0.16	0.06	0.06	0.01
Sb	40.25	39.84	38.39	37.53	39.43	34.97	35.95	33.57
Pb	24.61	24.49	31.17	25.37	25.88	7.25	6.8	4.86
SiO ₂	3.64	3.72	3.27	3.04	3.42	1.07	0.81	0.47
SO ₃	0.13	0.05	0.1	0.13	0.08	0.13	0.15	0.08
Fe ₂ O ₃	1.56	1.74	1.79	1.72	1.59	25.43	29.53	36.24
Sb ₂ O ₅	53.53	52.99	51.06	49.91	52.44	46.51	47.81	44.65
PbO	26.58	26.45	33.66	27.4	27.95	7.83	7.34	5.25
Total:	85.44	84.95	89.88	82.2	85.48	80.97	85.64	86.69
Mineral:	Bind	Bind	Bind	Bind	Bind	new	new	new
Pb:Fe ratio	6.09	5.41	6.72	5.70	6.28	0.11	0.09	0.05

Analysis No.	7e	9	9a	11	12	13	14	15
Si	0.33	0.27	0.23	0.27	0.23	0.29	0.26	0.68
S	0.02	0.05	0.05	0.03	0.05	0.05	0.03	0.04
Cl	0.01	0	0.02	0.01	0	0.01	0	0.02
Fe	22.26	23.53	25.44	24.86	24.48	22.67	23.23	12.46
Ag	0.08	0	0.04	0.02	0.01	0.06	0.12	0.11
Sb	34.55	34.09	33.15	33.04	34.16	34.72	34.33	36.42
Pb	7.53	4.7	4.62	5.3	4.42	9.18	7.58	11.95
SiO ₂	0.71	0.58	0.49	0.58	0.49	0.62	0.56	1.26
SO ₃	0.05	0.13	0.13	0.08	0.13	0.13	0.08	0.08
Fe ₂ O ₃	31.83	33.65	36.38	35.55	35.01	32.42	33.22	22.61
Sb ₂ O ₅	45.95	45.34	44.09	43.94	45.43	46.18	45.66	46.36
PbO	8.13	5.08	4.99	5.72	4.77	9.91	8.19	7.3
Total:	86.67	84.78	86.08	85.87	85.83	89.26	87.71	77.61
Mineral:	new							
Pb:Fe ratio	0.09	0.05	0.05	0.06	0.05	0.11	0.09	0.26

Analysis No.	16	17	18	19	20	21	22	24
Si	0.59	0.53	0.95	0.39	1.34	0.29	0.32	0.25
S	0.03	0.04	0.34	0.04	0.01	0.03	0.03	0.03
Cl	0.01	0.05	0.18	0.01	0.04	0	0	0.03
Fe	15.81	19.12	12.14	19.71	6.1	22.77	21.7	24.2
Ag	0.06	0.17	1.06	0	0.04	0.04	0.07	0.08
Sb	34.86	34.45	34.78	35.15	38.24	34.4	34.88	34.13
Pb	6.76	12.17	14.75	10.5	25.1	5.19	8.46	10.82
SiO2	1.26	1.13	2.03	0.83	2.87	0.62	0.68	0.54
SO3	0.08	0.1	0.85	0.1	0.03	0.08	0.08	0.08
Fe2O3	22.61	27.34	17.36	28.19	8.72	32.56	31.03	34.61
Sb2O5	46.36	45.82	46.26	46.75	50.86	45.75	46.39	45.39
PbO	7.3	13.14	15.93	11.34	27.11	5.61	9.14	11.69
Total:	77.61	87.53	82.43	87.21	89.59	84.62	87.32	92.31
Mineral:	new	new	new	new	Bind	new	new	new
Pb:Fe ratio	0.12	0.17	0.33	0.14	1.11	0.06	0.11	0.12

Analysis No.	25	26	27	28
Si	1.59	1.7	0.51	1.62
S	0.03	0.02	0.02	0.04
Cl	0.03	0.04	0.01	0.04
Fe	1.23	1.16	17.17	1.28
Ag	0.23	0.11	0	0.12
Sb	39.13	39.15	36.41	39.08
Pb	25.79	24.97	10.86	25.69
SiO2	3.4	3.64	1.09	3.47
SO3	0.08	0.05	0.05	0.1
Fe2O3	1.76	1.66	24.55	1.83
Sb2O5	52.04	52.07	48.43	51.98
PbO	27.85	26.97	11.73	27.75
Total:	85.13	84.39	85.85	85.13
Mineral:	Bind	Bind	new	Bind
	5.65	5.80	0.17	5.41

APPENDIX 2

Bayley Park Soil Geochemistry Assays.

Eastings	Northing	Analyte	Sample ID	Al %	As ppm	Ba ppm	Ca %	Co ppm	Cr ppm	Cu ppm	Fe %	Mg %	Mn ppm	Mo ppm	Ni ppm	Pb ppm
391310	624278	B1006	BPBS5	0.001	2	1	0.01	1	1	1	0.01	0.01	5	1	1	2
391306	624295	B1005	BPBS4	0.846	112	92	0.08	2	7	12	2.19	0.08	194	1	4	13
391310	624316	B1004	BPBS3	0.901	18	106	0.1	2	12	7	1.59	0.13	172	1	4	10
391310	624337	B1003	BPBS2	1.015	22	91	0.14	3	10	19	1.55	0.14	179	1	4	11
391310	624356	B1002	BPBS1	1.02	14	73	0.06	2	15	12	1.64	0.13	139	1	3	11
391308	624373	B1001	BPB0	0.906	109	122	0.2	4	8	169	1.85	0.08	281	3	5	21
391312	624395	B1007	BPBN1	1.635	25	180	0.16	3	12	16	1.87	0.14	531	1	7	15
391308	624415	B1008	BPBN2	1.15	27	102	0.09	2	9	9	2.07	0.12	146	1	4	14
391307	624439	B1009	BPBN3	1.215	23	161	0.19	3	8	12	1.86	0.19	545	1	5	14
391310	624458	B1010	BPBN4	1.345	13	165	0.15	4	10	10	1.7	0.23	504	1	6	15
391311	624477	B1011	BPBN5	1.475	16	179	0.14	4	11	17	2.33	0.27	380	1	6	18
391236	624361	B1016	BPAS4	1.21	11	161	0.18	3	11	12	1.98	0.25	345	1	5	14
391236	624401	B1014	BPAS2	1.075	9	243	0.24	6	11	14	1.04	0.12	464	0.5	6	12
391236	624423	B1013	BPAS1	1.03	9	59	0.04	2	10	9	1.23	0.12	75	1	3	8
391234	624439	B1012	BPA0	0.925	22	98	0.06	2	9	5	1.22	0.13	236	0.5	3	12
391234	624461	B1018	BPAN1	0.863	13	114	0.14	3	8	11	1.23	0.12	293	1	4	11
391231	624481	B1019	BPAN2	1.3	8	185	0.17	8	12	15	1.42	0.18	776	1	6	17
391228	624500	B1020	BPAN3	1.35	7	135	0.18	4	13	9	1.61	0.25	288	1	5	13
391228	624521	B1021	BPAN4	0.985	12	97	0.09	4	9	9	1.47	0.15	167	0.5	4	10
391530	624218	B1028	BPCS5	0.769	8	87	0.08	2	12	5	1.23	0.1	131	1	3	10
391527	624254	B1026	BPCS3	1.015	22	130	0.1	5	13	8	1.5	0.14	328	1	7	12
391527	624275	B1025	BPCS2	1.24	32	206	0.23	6	10	12	1.86	0.11	754	1	6	18
391524	624298	B1024	BPCS1	1.065	91	170	0.26	4	24	10	1.82	0.09	454	1	6	14
391522	624312	B1023	BPC0	1.155	38	110	0.18	4	9	11	2.17	0.13	258	1	7	13
391522	624332	B1029	BPCN1	1.27	22	127	0.04	4	18	8	1.83	0.2	256	1	7	12
391522	624353	B1030	BPCN2	1.475	13	208	0.14	7	28	13	1.52	0.25	449	1	15	16
391519	624371	B1031	BPCN3	0.991	21	148	0.12	5	12	11	1.51	0.12	361	1	6	13
391521	624413	B1033	BPCN5	1.02	44	157	0.11	4	14	7	1.73	0.16	226	1	4	15
				0.576	22	76	0.1	2	16	3	1.01	0.06	239	1	2	8

Easting	Northing	Analyte	Sample ID	S	Zn	Au	Ag	Bi	Cd	Hg	Sb	Se	Sn	Te	Tl	W
				%	ppm	ppm										
391310	624278	B1006	BPBS5	0.01	2	0.001	0.02	0.02	0.02	0.02	0.1	0.5	0.1	0.02	0.02	0.1
391306	624295	B1005	BPBS4	0.02	30	0.002	0.03	0.33	0.03	0.03	44.2	0.25	0.3	0.03	0.09	1.4
391310	624316	B1004	BPBS3	0.03	26	0.001	0.03	0.26	0.03	0.05	12.6	0.25	0.4	0.02	0.14	0.2
391310	624337	B1003	BPBS2	0.03	37	0.002	0.03	0.27	0.03	0.04	12.8	0.25	0.3	0.02	0.16	1.6
391310	624356	B1002	BPBS1	0.03	27	0.002	0.03	0.28	0.03	0.02	16.4	0.25	0.5	0.02	0.17	0.05
391308	624373	B1001	BPB0	0.07	63	0.015	0.12	0.41	0.13	0.08	187.5	0.25	0.4	0.04	0.13	2.6
391312	624395	B1007	BPBN1	0.04	44	0.003	0.04	0.32	0.06	0.05	116	0.25	0.5	0.03	0.2	0.1
391308	624415	B1008	BPBN2	0.03	35	0.001	0.03	0.33	0.04	0.04	43.7	0.25	0.4	0.03	0.14	0.1
391307	624439	B1009	BPBN3	0.04	41	0.001	0.03	0.29	0.04	0.03	54.3	0.25	0.4	0.03	0.17	0.1
391310	624458	B1010	BPBN4	0.03	39	0.001	0.04	0.33	0.05	0.05	15.7	0.25	0.6	0.03	0.17	0.05
391311	624477	B1011	BPBN5	0.03	54	0.0005	0.04	0.36	0.04	0.03	13.9	0.25	0.6	0.03	0.16	0.2
391236	624361	B1016	BPAS4	0.03	41	0.0005	0.04	0.34	0.03	0.02	5.7	0.25	0.7	0.03	0.13	0.05
391236	624401	B1014	BPAS2	0.04	22	0.0005	0.04	0.2	0.05	0.05	11.4	0.25	0.5	0.01	0.09	2.4
391236	624423	B1013	BPAS1	0.02	22	0.0005	0.03	0.21	0.01	0.03	7.1	0.25	0.3	0.02	0.11	2.3
391234	624439	B1012	BPA0	0.03	20	0.002	0.02	0.14	0.02	0.03	90.8	0.25	0.4	0.01	0.12	0.1
391234	624461	B1018	BPAN1	0.04	25	0.0005	0.03	0.18	0.05	0.02	40.9	0.25	0.4	0.02	0.11	0.7
391231	624481	B1019	BPAN2	0.04	38	0.0005	0.03	0.25	0.05	0.03	2.7	0.25	0.6	0.02	0.13	0.4
391228	624500	B1020	BPAN3	0.03	36	0.0005	0.03	0.25	0.05	0.02	1.8	0.25	0.8	0.02	0.15	0.05
391228	624521	B1021	BPAN4	0.02	25	0.0005	0.03	0.22	0.02	0.02	1.8	0.25	0.4	0.02	0.11	1.2
391530	624218	B1028	BPCS5	0.03	20	0.0005	0.02	0.2	0.03	0.02	1.3	0.25	0.4	0.02	0.08	0.05
391527	624254	B1026	BPCS3	0.03	21	0.0005	0.04	0.28	0.05	0.04	19.1	0.25	0.5	0.02	0.12	2.3
391527	624275	B1025	BPCS2	0.04	32	0.001	0.04	0.35	0.06	0.06	26.1	0.5	0.4	0.03	0.08	1.9
391524	624298	B1024	BPCS1	0.04	27	0.002	0.03	0.32	0.09	0.05	26.4	0.5	0.3	0.03	0.06	0.4
391522	624312	B1023	BPC0	0.03	36	0.001	0.02	0.28	0.05	0.04	44.8	0.5	0.3	0.03	0.11	1.2
391522	624332	B1029	BPCN1	0.03	35	0.001	0.03	0.26	0.03	0.04	17.1	0.25	0.4	0.03	0.14	0.1
391522	624353	B1030	BPCN2	0.04	34	0.001	0.04	0.24	0.1	0.06	10.6	0.6	0.6	0.02	0.13	0.05
391522	624371	B1031	BPCN3	0.04	26	0.002	0.04	0.25	0.09	0.04	28.8	0.25	0.4	0.02	0.11	3.4
391519	624371	B1033	BPCN5	0.03	27	0.003	0.04	0.29	0.07	0.03	44.4	0.25	0.4	0.03	0.15	0.1
391521	624413	B1033	BPCN5	0.03	9	0.001	0.03	0.15	0.04	0.02	46	0.25	0.3	0.02	0.08	0.05

APPENDIX 3

Refinement Details for Unit Cell Data of Mineral Phases.

Synthetic Bottinoite

Refined Cell Dimensions by Cohen's Method of Least Squares

Refinement Code: 2: No correction to 2Theta

Hexagonal (4)

Wavelength = 1.540598 Å

Trial Cell Dimensions

a = 16.06000 Å, b = 16.06000 Å, c = 9.79200 Å,

Alpha = 90.000 Deg., Beta = 90.000 Deg., Gamma = 120.000 Deg.

Refined Cell Dimensions

a = 16.06950 Å, b = 16.06950 Å, c = 9.80048 Å,

Std. Errors in a, b and c are .00173, .00173 and .00103 Å

Alpha = 90.000 Deg., Beta = 90.000 Deg., Gamma = 120.000 Deg.

Std. Errors in Alpha, Beta and Gamma are .000, .000 and .000 Deg.

Volume = 2191.707 Cu Å, Std. Error = .423 Cu Å

c/a = .60988

S.D. c/a = .00009

Coefficients of Correction Function $A + B\cos\theta + C\sin 2\theta$ are:

A = .0000 B = .0000 C = .0000

S.D. A = .0000 S.D. B = .0000 S.D. C = .0000

Zero = .000 Deg 2Th, S.D. Zero = .000 Deg 2Th

SSD = .000 mm, S.D. SSD = .000 mm

mu = .0 1/mm S.D. mu = .0 1/mm

d-Spacings, etc.

n = 45

h	k	l	2THobs	2THcor	2THcal	Del2TH	VcX10	Do A	Dc A	ED A
1	1	0	10.980	10.980	11.003	.023	6	8.05146	8.03475	-.01671
1	1	-1	14.220	14.220	14.243	.023	8	6.22340	6.21352	-.00987
0	0	2	18.062	18.062	18.088	.026	12	4.90734	4.90024	-.00710
3	0	0	19.093	19.093	19.117	.024	11	4.64461	4.63886	-.00574
0	3	1	21.158	21.158	21.173	.015	7	4.19573	4.19289	-.00284
2	0	2	22.100	22.100	22.170	.070	38	4.01897	4.00646	-.01252
2	2	-1	23.880	23.880	23.920	.040	23	3.72328	3.71719	-.00609
3	0	2	26.422	26.422	26.436	.014	9	3.37055	3.36879	-.00177
0	0	3	27.260	27.260	27.277	.017	11	3.26881	3.26683	-.00199
2	2	-2	28.700	28.700	28.712	.012	8	3.10799	3.10676	-.00123
1	3	-2	29.400	29.400	29.434	.034	24	3.03557	3.03212	-.00344
4	1	-1	30.780	30.780	30.799	.019	14	2.90254	2.90078	-.00176
3	3	0	33.436	33.436	33.430	-.006	-4	2.67780	2.67825	.00045
3	3	-1	34.669	34.669	34.694	.025	21	2.58533	2.58352	-.00182
2	2	-3	35.400	35.400	35.386	-.014	-12	2.53360	2.53459	.00099
0	0	4	36.640	36.640	36.648	.008	7	2.45065	2.45012	-.00053
1	0	4	37.280	37.280	37.232	-.048	-42	2.41004	2.41301	.00297
3	3	-2	38.265	38.265	38.267	.002	1	2.35024	2.35014	-.00010
6	0	0	38.790	38.790	38.793	.003	3	2.31963	2.31943	-.00020
6	0	1	39.900	39.900	39.910	.010	9	2.25762	2.25708	-.00053
5	1	-2	40.460	40.460	40.481	.021	19	2.22765	2.22657	-.00108
3	0	4	41.644	41.644	41.654	.010	10	2.16701	2.16650	-.00052
6	0	2	43.120	43.120	43.115	-.005	-5	2.09619	2.09645	.00025
3	3	-3	43.680	43.680	43.667	-.013	-12	2.07061	2.07117	.00057

5	2	-2	44.600	44.600	44.634	.034	35	2.03001	2.02853	-.00148
0	0	5	46.300	46.300	46.281	-.019	-19	1.95935	1.96010	.00074
6	1	-2	46.660	46.660	46.599	-.061	-64	1.94507	1.94746	.00239
1	4	-4	47.660	47.660	47.652	-.008	-9	1.90657	1.90688	.00032
6	0	3	48.100	48.100	48.071	-.029	-32	1.89015	1.89123	.00108
5	2	-3	49.460	49.460	49.471	.011	12	1.84131	1.84092	-.00039
3	3	-4	50.443	50.443	50.441	-.002	-2	1.80771	1.80778	.00007
3	6	0	52.117	52.117	52.123	.006	7	1.75351	1.75333	-.00019
6	3	-1	53.020	53.020	53.015	-.005	-6	1.72576	1.72592	.00017
6	0	4	54.427	54.427	54.428	.001	1	1.68442	1.68439	-.00003
6	3	-2	55.623	55.623	55.629	.006	7	1.65100	1.65083	-.00017
0	0	6	56.260	56.260	56.275	.015	18	1.63381	1.63341	-.00040
1	0	6	56.700	56.700	56.696	-.004	-4	1.62217	1.62228	.00010
1	1	6	57.520	57.520	57.532	.012	15	1.60098	1.60067	-.00031
5	5	-1	58.140	58.140	58.124	-.016	-19	1.58538	1.58577	.00040
9	0	0	59.760	59.760	59.757	-.003	-4	1.54621	1.54629	.00008
2	8	1	61.760	61.760	61.775	.015	19	1.50085	1.50052	-.00033
9	0	2	62.980	62.980	62.983	.003	4	1.47468	1.47461	-.00007
5	2	5	63.140	63.140	63.119	-.021	-28	1.47133	1.47177	.00045
4	1	6	64.740	64.740	64.752	.012	16	1.43878	1.43853	-.00025
3	6	4	65.400	65.400	65.400	.000	0	1.42585	1.42585	.00000

Sum Delta 2Theta = .257
 S.D. Delta 2Theta = .023
 Sum Vc X 100,000 = 116.0

Synthetic Brandholzite

Refined Cell Dimensions by Cohen s Method of Least Squares

Refinement Code: 2: No correction to 2Theta

Hexagonal (4)

Wavelength = 1.540600 A

Trial Cell Dimensions

a = 16.11300 A, b = 16.11300 A, c = 9.86800 A,

Alpha = 90.000 Deg., Beta = 90.000 Deg., Gamma = 120.000 Deg.

Refined Cell Dimensions

a = 16.12395 A, b = 16.12395 A, c = 9.87412 A,

Std. Errors in a, b and c are .00112, .00112 and .00053 A

Alpha = 90.000 Deg., Beta = 90.000 Deg., Gamma = 120.000 Deg.

Std. Errors in Alpha, Beta and Gamma are .000, .000 and .000 Deg.

Volume = 2223.166 Cu A, Std. Error = .256 Cu A

c/a = .61239

S.D. c/a = .00005

Coefficients of Correction Function A + B Cos Theta + C Sin 2 Theta are:

A = .0000 B = .0000 C = .0000

S.D. A = .0000 S.D. B = .0000 S.D. C = .0000

Zero = .000 Deg 2Th, S.D. Zero = .000 Deg 2Th

SSD = .000 mm, S.D. SSD = .000 mm

mu = .0 1/mm S.D. mu = .0 1/mm

d-Spacings, etc.

n = 53

h	k	l	2THobs	2THcor	2THcal	Del2TH	VcX10	Do A	Dc A	ED A
0	0	1	8.918	8.918	8.949	.031	6	9.90794	9.87412	-.03382
1	0	1	10.942	10.942	10.965	.023	6	8.07934	8.06212	-.01723
1	1	1	14.153	14.153	14.171	.018	6	6.25272	6.24484	-.00787
0	0	2	17.924	17.924	17.952	.028	12	4.94481	4.93706	-.00775
3	0	0	19.037	19.037	19.052	.015	7	4.65815	4.65458	-.00357
3	0	1	21.071	21.071	21.084	.013	7	4.21286	4.21025	-.00262
2	0	2	22.026	22.026	22.033	.007	3	4.03231	4.03106	-.00126
2	2	1	23.814	23.814	23.824	.010	5	3.73345	3.73198	-.00147
2	1	2	24.643	24.643	24.672	.029	18	3.60970	3.60547	-.00423
3	0	2	26.284	26.284	26.293	.009	6	3.38794	3.38675	-.00119
0	0	3	27.053	27.053	27.070	.017	11	3.29336	3.29137	-.00198
2	2	2	28.571	28.571	28.565	-.006	-4	3.12174	3.12242	.00069
1	1	3	29.281	29.281	29.285	.004	3	3.04764	3.04721	-.00043
4	1	1	30.677	30.677	30.681	.004	3	2.91205	2.91165	-.00041
3	0	3	33.310	33.310	33.313	.003	2	2.68764	2.68737	-.00027
1	4	2	34.556	34.556	34.563	.007	5	2.59353	2.59302	-.00051
2	2	3	35.171	35.171	35.173	.002	1	2.54958	2.54946	-.00012
0	0	4	36.380	36.380	36.365	-.015	-12	2.46757	2.46853	.00096
3	3	2	38.096	38.096	38.095	-.001	0	2.36028	2.36032	.00004
6	0	0	38.655	38.655	38.657	.002	2	2.32742	2.32729	-.00013
6	0	1	39.759	39.759	39.760	.001	1	2.26530	2.26522	-.00008
1	4	3	40.305	40.305	40.302	-.003	-2	2.23586	2.23602	.00015
3	0	4	41.360	41.360	41.368	.008	8	2.18124	2.18082	-.00042
6	0	2	42.925	42.925	42.928	.003	3	2.10526	2.10512	-.00014
3	3	3	43.437	43.437	43.437	.000	0	2.08163	2.08161	-.00001
5	2	2	44.441	44.441	44.443	.002	1	2.03690	2.03683	-.00007
4	0	4	44.920	44.920	44.938	.018	18	2.01629	2.01553	-.00076
4	4	1	45.914	45.914	45.918	.004	3	1.97492	1.97477	-.00015
3	2	4	46.380	46.380	46.400	.020	21	1.95616	1.95535	-.00081
1	1	5	47.356	47.356	47.355	-.001	0	1.91810	1.91812	.00002
6	0	3	47.818	47.818	47.829	.011	11	1.90064	1.90024	-.00039
4	4	2	48.740	48.740	48.763	.023	25	1.86682	1.86599	-.00083
5	0	4	49.227	49.227	49.224	-.003	-2	1.84948	1.84957	.00009
3	3	4	50.131	50.131	50.139	.008	9	1.81823	1.81795	-.00028
6	3	0	51.936	51.936	51.934	-.002	-2	1.75920	1.75927	.00007
1	7	2	52.810	52.810	52.814	.004	5	1.73213	1.73200	-.00013
6	0	4	54.115	54.115	54.116	.001	0	1.69340	1.69337	-.00002
6	3	2	55.398	55.398	55.397	-.001	0	1.65718	1.65720	.00002
6	1	4	57.081	57.081	57.075	-.006	-7	1.61225	1.61241	.00016
3	3	5	57.891	57.891	57.901	.010	12	1.59160	1.59134	-.00026
2	1	6	58.720	58.720	58.720	.000	0	1.57109	1.57108	-.00001
3	0	6	59.526	59.526	59.533	.007	8	1.55173	1.55156	-.00017
5	5	2	60.340	60.340	60.340	.000	0	1.53273	1.53272	-.00001
2	2	6	60.732	60.732	60.739	.007	9	1.52377	1.52360	-.00017
3	1	6	61.160	61.160	61.138	-.022	-27	1.51413	1.51461	.00048
6	0	5	61.514	61.514	61.536	.022	28	1.50626	1.50577	-.00049
9	0	2	62.716	62.716	62.721	.005	5	1.48025	1.48016	-.00010
2	8	2	63.910	63.910	63.891	-.019	-24	1.45545	1.45582	.00038
4	1	6	64.277	64.277	64.278	.001	1	1.44802	1.44800	-.00002
3	6	4	65.053	65.053	65.050	-.003	-3	1.43261	1.43266	.00005
3	3	6	66.576	66.576	66.579	.003	3	1.40349	1.40344	-.00005
1	1	7	67.360	67.360	67.336	-.024	-32	1.38904	1.38948	.00044
8	2	3	67.740	67.740	67.715	-.025	-34	1.38217	1.38262	.00045

Sum Delta 2Theta = .254
 S.D. Delta 2Theta = .013
 Sum Vc X 100,000 = 134.8

Bindheimite Pb₂Sb₂O₇ Pb:Sb Solution Ratio 1:2

Sample number: PBSB2
 Refined Cell Dimensions by Cohen s Method of Least Squares
 Refinement Code: 2: No correction to 2Theta
 Cubic (7)
 Wavelength = 1.540598 A
 Trial Cell Dimensions
 a = 10.06000 A, b = 10.06000 A, c = 10.06000 A,
 Alpha = 90.000 Deg., Beta = 90.000 Deg., Gamma = 90.000 Deg.
 Refined Cell Dimensions
 a = 10.41692 A, b = 10.41692 A, c = 10.41692 A,
 Std. Errors in a, b and c are .00246, .00246 and .00246 A
 Alpha = 90.000 Deg., Beta = 90.000 Deg., Gamma = 90.000 Deg.
 Std. Errors in Alpha, Beta and Gamma are .000, .000 and .000 Deg.
 Volume = 1130.364 Cu A, Std. Error = .801 Cu A
 Coefficients of Correction Function A + BCosTheta + CSin2Theta are:
 A = .0000 B = .0000 C = .0000
 S.D. A = .0000 S.D. B = .0000 S.D. C = .0000
 Zero = .000 Deg 2Th, S.D. Zero = .000 Deg 2Th
 SSD = .000 mm, S.D. SSD = .000 mm
 mu = .0 1/mm S.D. mu = .0 1/mm
 d-Spacings, etc.
 n = 12

h	k	l	2THobs	2THcor	2THcal	Del2TH	VcX10	Do A	Dc A	ED A
1	1	1	14.640	14.640	14.717	.077	28	6.04579	6.01421	-.03158
3	1	1	28.500	28.500	28.394	-.106	-74	3.12935	3.14082	.01147
2	2	2	29.660	29.660	29.685	.025	17	3.00955	3.00711	-.00244
4	0	0	34.320	34.320	34.410	.090	74	2.61082	2.60423	-.00659
4	2	2	42.440	42.440	42.479	.039	38	2.12819	2.12635	-.00185
5	1	1	45.220	45.220	45.193	-.027	-28	2.00361	2.00474	.00113
4	4	0	49.400	49.400	49.455	.055	61	1.84341	1.84147	-.00194
5	3	1	51.920	51.920	51.886	-.034	-39	1.75970	1.76078	.00108
6	2	2	58.720	58.720	58.748	.028	35	1.57109	1.57041	-.00068
4	4	4	61.600	61.600	61.637	.037	47	1.50436	1.50355	-.00081
7	1	1	63.760	63.760	63.752	-.008	-9	1.45851	1.45866	.00015
7	3	1	69.280	69.280	69.221	-.059	-80	1.35516	1.35617	.00101

Sum Delta 2Theta = .117
 S.D. Delta 2Theta = .059
 Sum Vc X 100,000 = 71.5

Bindheimite Pb₂Sb₂O₇ Pb:Sb Solution Ratio 1:1

Sample number: PBSB4
 Refined Cell Dimensions by Cohen s Method of Least Squares
 Refinement Code: 2: No correction to 2Theta
 Cubic (7)

Wavelength = 1.540598 A
 Trial Cell Dimensions
 a = 10.06000 A, b = 10.06000 A, c = 10.06000 A,
 Alpha = 90.000 Deg., Beta = 90.000 Deg., Gamma = 90.000 Deg.
 Refined Cell Dimensions
 a = 10.45198 A, b = 10.45198 A, c = 10.45198 A,
 Std. Errors in a, b and c are .00637, .00637 and .00637 A
 Alpha = 90.000 Deg., Beta = 90.000 Deg., Gamma = 90.000 Deg.
 Std. Errors in Alpha, Beta and Gamma are .000, .000 and .000 Deg.
 Volume = 1141.814 Cu A, Std. Error = 2.086 Cu A
 Coefficients of Correction Function $A + B\cos\theta + C\sin^2\theta$ are:
 A = .0000 B = .0000 C = .0000
 S.D. A = .0000 S.D. B = .0000 S.D. C = .0000
 Zero = .000 Deg 2Th, S.D. Zero = .000 Deg 2Th
 SSD = .000 mm, S.D. SSD = .000 mm
 mu = .0 1/mm S.D. mu = .0 1/mm
 d-Spacings, etc.
 n = 9

h	k	l	2THobs	2THcor	2THcal	Del2TH	VcX10	Do A	Dc A	ED A
1	1	1	14.740	14.740	14.668	-.072	-27	6.00500	6.03445	.02946
2	2	2	29.540	29.540	29.583	.043	31	3.02150	3.01723	-.00427
4	0	0	34.240	34.240	34.291	.051	41	2.61674	2.61299	-.00374
3	3	1	37.600	37.600	37.477	-.123	-110	2.39026	2.39785	.00759
5	1	1	44.960	44.960	45.033	.073	76	2.01459	2.01148	-.00310
4	4	0	49.480	49.480	49.279	-.201	-224	1.84061	1.84767	.00705
5	3	1	51.660	51.660	51.699	.039	44	1.76795	1.76671	-.00124
6	2	2	58.500	58.500	58.532	.032	39	1.57647	1.57569	-.00078
4	4	4	61.360	61.360	61.408	.048	61	1.50967	1.50861	-.00106

Sum Delta 2Theta = -.112
 S.D. Delta 2Theta = .097
 Sum Vc X 100,000 = -67.1

Roméite Ca₂Sb₂O₇, Ca:Sb Solution Ratio 1:2

Sample number: CASB2
 Refined Cell Dimensions by Cohen s Method of Least Squares
 Refinement Code: 2: No correction to 2Theta
 Cubic (7)
 Wavelength = 1.540598 A
 Trial Cell Dimensions
 a = 10.06000 A, b = 10.06000 A, c = 10.06000 A,
 Alpha = 90.000 Deg., Beta = 90.000 Deg., Gamma = 90.000 Deg.
 Refined Cell Dimensions
 a = 10.27705 A, b = 10.27705 A, c = 10.27705 A,
 Std. Errors in a, b and c are .00199, .00199 and .00199 A
 Alpha = 90.000 Deg., Beta = 90.000 Deg., Gamma = 90.000 Deg.
 Std. Errors in Alpha, Beta and Gamma are .000, .000 and .000 Deg.
 Volume = 1085.440 Cu A, Std. Error = .629 Cu A
 Coefficients of Correction Function $A + B\cos\theta + C\sin^2\theta$ are:
 A = .0000 B = .0000 C = .0000
 S.D. A = .0000 S.D. B = .0000 S.D. C = .0000
 Zero = .000 Deg 2Th, S.D. Zero = .000 Deg 2Th
 SSD = .000 mm, S.D. SSD = .000 mm

mu = .0 1/mm S.D. mu = .0 1/mm

d-Spacings, etc.

n = 11

h	k	l	2THobs	2THcor	2THcal	Del2TH	VcX10	Do A	Dc A	ED A
1	1	1	14.842	14.842	14.919	.077	28	5.96396	5.93346	-.03050
3	1	1	28.802	28.802	28.788	-.014	-9	3.09722	3.09865	.00143
2	2	2	30.042	30.042	30.098	.056	41	2.97214	2.96673	-.00541
4	0	0	34.842	34.842	34.893	.051	42	2.57289	2.56926	-.00363
3	3	1	38.102	38.102	38.139	.037	33	2.35991	2.35772	-.00220
5	1	1	45.842	45.842	45.843	.001	0	1.97786	1.97782	-.00004
4	4	0	50.222	50.222	50.175	-.047	-53	1.81514	1.81674	.00160
5	3	1	52.682	52.682	52.646	-.036	-42	1.73603	1.73714	.00111
6	2	2	59.662	59.662	59.628	-.034	-43	1.54852	1.54932	.00081
4	4	4	62.542	62.542	62.570	.028	35	1.48395	1.48336	-.00059
7	1	1	64.702	64.702	64.725	.023	30	1.43953	1.43908	-.00045

Sum Delta 2Theta = .141

S.D. Delta 2Theta = .044

Sum Vc X 100,000 = 65.1

Roméite Ca₂Sb₂O₇ Ca:Sb Slution Ratio 1:1

Sample number: CASB4

Refined Cell Dimensions by Cohen s Method of Least Squares

Refinement Code: 2: No correction to 2Theta

Cubic (7)

Wavelength = 1.540598 A

Trial Cell Dimensions

a = 10.06000 A, b = 10.06000 A, c = 10.06000 A,

Alpha = 90.000 Deg., Beta = 90.000 Deg., Gamma = 90.000 Deg.

Refined Cell Dimensions

a = 10.28866 A, b = 10.28866 A, c = 10.28866 A,

Std. Errors in a, b and c are .00222, .00222 and .00222 A

Alpha = 90.000 Deg., Beta = 90.000 Deg., Gamma = 90.000 Deg.

Std. Errors in Alpha, Beta and Gamma are .000, .000 and .000 Deg.

Volume = 1089.121 Cu A, Std. Error = .704 Cu A

Coefficients of Correction Function A + BCosTheta + CSin2Theta are:

A = .0000 B = .0000 C = .0000

S.D. A = .0000 S.D. B = .0000 S.D. C = .0000

Zero = .000 Deg 2Th, S.D. Zero = .000 Deg 2Th

SSD = .000 mm, S.D. SSD = .000 mm

mu = .0 1/mm S.D. mu = .0 1/mm

d-Spacings, etc.

n = 12

h	k	l	2THobs	2THcor	2THcal	Del2TH	VcX10	Do A	Dc A	ED A
1	1	1	14.780	14.780	14.902	.122	45	5.98883	5.94016	-.04868
3	1	1	28.700	28.700	28.755	.055	39	3.10799	3.10215	-.00585
2	2	2	29.980	29.980	30.063	.083	61	2.97815	2.97008	-.00807
4	0	0	34.860	34.860	34.852	-.008	-6	2.57160	2.57216	.00056
3	3	1	38.140	38.140	38.094	-.046	-41	2.35765	2.36038	.00273
4	2	2	42.980	42.980	43.034	.054	54	2.10270	2.10016	-.00253
5	1	1	45.780	45.780	45.788	.008	8	1.98039	1.98005	-.00034
4	4	0	50.180	50.180	50.114	-.066	-74	1.81657	1.81879	.00223

5	3	1	52.560	52.560	52.582	.022	25	1.73977	1.73910	-.00067
6	2	2	59.580	59.580	59.554	-.026	-33	1.55045	1.55107	.00062
4	4	4	62.500	62.500	62.491	-.009	-11	1.48485	1.48504	.00019
7	1	1	64.620	64.620	64.643	.023	30	1.44116	1.44070	-.00046

Sum Delta 2Theta = .213
 S.D. Delta 2Theta = .057
 Sum Vc X 100,000 = 98.2

Natural Stibiconite from the Razorback Mine

Refined Cell Dimensions by Cohen s Method of Least Squares

Refinement Code: 2: No correction to 2Theta

Cubic (7)

Wavelength = 1.540598 A

Trial Cell Dimensions

a = 10.06000 A, b = 10.06000 A, c = 10.06000 A,

Alpha = 90.000 Deg., Beta = 90.000 Deg., Gamma = 90.000 Deg.

Refined Cell Dimensions

a = 10.26091 A, b = 10.26091 A, c = 10.26091 A,

Std. Errors in a, b and c are .00200, .00200 and .00200 A

Alpha = 90.000 Deg., Beta = 90.000 Deg., Gamma = 90.000 Deg.

Std. Errors in Alpha, Beta and Gamma are .000, .000 and .000 Deg.

Volume = 1080.334 Cu A, Std. Error = .632 Cu A

Coefficients of Correction Function $A + B\cos\theta + C\sin 2\theta$ are:

A = .0000 B = .0000 C = .0000

S.D. A = .0000 S.D. B = .0000 S.D. C = .0000

Zero = .000 Deg 2Th, S.D. Zero = .000 Deg 2Th

SSD = .000 mm, S.D. SSD = .000 mm

mu = .0 1/mm S.D. mu = .0 1/mm

d-Spacings, etc.

n = 13

h	k	l	2THobs	2THcor	2THcal	Del2TH	VcX10	Do A	Dc A	ED A
1	1	1	14.860	14.860	14.942	.082	31	5.95677	5.92414	-.03263
3	1	1	28.820	28.820	28.835	.015	10	3.09532	3.09378	-.00154
2	2	2	30.080	30.080	30.147	.067	49	2.96847	2.96207	-.00640
4	0	0	34.920	34.920	34.949	.029	24	2.56732	2.56523	-.00209
3	3	1	38.160	38.160	38.201	.041	37	2.35646	2.35402	-.00245
4	2	2	43.160	43.160	43.157	-.003	-3	2.09434	2.09450	.00016
5	1	1	45.920	45.920	45.919	-.001	0	1.97468	1.97471	.00004
4	4	0	50.320	50.320	50.259	-.061	-68	1.81184	1.81389	.00205
5	3	1	52.700	52.700	52.735	.035	40	1.73548	1.73441	-.00107
5	3	3	59.020	59.020	58.980	-.040	-49	1.56382	1.56477	.00096
6	2	2	59.780	59.780	59.731	-.049	-62	1.54574	1.54689	.00115
4	4	4	62.660	62.660	62.679	.019	24	1.48144	1.48104	-.00040
7	1	1	64.800	64.800	64.839	.039	52	1.43759	1.43682	-.00077

Sum Delta 2Theta = .174
 S.D. Delta 2Theta = .045
 Sum Vc X 100,000 = 85.6